Journal of Engineering Mathematics **44:** 395–448, 2002.

Survey of the mathematical theory of fish locomotion

J.A. SPARENBERG
Mathematics Department, University of Groningen, P.O. Box 800, 9700 AV Groningen, The Netherlands

Received 1 October 2001; accepted in revised form 21 June 2002

Abstract. In this paper an attempt is made to give a survey of the mathematical approach to the description of the swimming of fish. This type of investigation is of interest because it gives insight in the fundamentals of the interaction of the body of the fish and the fluid. Sir James Lighthill considered this problem in a very lively way by showing that simple ideas can be the nucleus of deep mathematical investigations. He and, besides him, T.Y. Wu can most probably be regarded as the founders of the hydrodynamical description of fish locomotion. They have stimulated many capable theoreticians to contribute to this rich field of beautiful problems. Of course, the mathematical investigations were stimulated by the many experimental discoveries already made earlier by prominent biologists.

Key words: fish locomotion, hydrodynamic propulsion, swimming.

Table of Contents

1. Introduction

This James Lighthill Memorial Paper bears only upon part of the many activities of Sir James Lighthill, namely upon the mathematical theory of the swimming of fish and cetaceans. It is well-known that M.J. Lighthill considered many aspects of fluid mechanics, as follows from his collected papers which are covered by four volumes [1]. Besides his mathematical approach to fish locomotion Lighthill went, as he says himself with the help of colleagues in zoology, deeply into the biological background of the different phenomena that he investigated. Along with Lighthill, Wu must also be mentioned as the author of a number of papers which contribute to the mathematical foundation of the subject.

We will now give a brief survey of the research on fish locomotion which started early in history. According to Alexander in 'The history of fish mechanics' [2], which we follow in a strongly abridged way, already Aristotle considers in some of his works the anatomy and locomotion of swimming creatures. After this, however, it took a long time before fish mechanics really made progress.

There was a real increase in research activities during the final stages of the 17th century. For instance research was carried out with respect to the swim bladder. At that time Torricelly had developed the mercury barometer and von Guericke had invented the air pump. By decreasing the pressure on the surface of the water in a vessel in which a fish was present, the bladder of the fish expanded, by which the fish rose to the surface and could not swim downwards. When the original pressure was restored, the fish sank to the bottom of the vessel since, as turned out by dissection, too little air was left in the bladder.

From about 1700–1800 research on fish was not making much progress. Its revival was due to the further development of apparatuses for measuring pressures and to the invention of photography and film by which the movements of the fish could be recorded. Some names are A. Moreau regarding measurements at the bladder and E.J. Marey for the recording of fish movements.

After 1910 until 1950 research was done, not only by zoologists, but also by engineers, which yielded a fruitful collaboration. For instance, wooden models of fish were towed through water and their resistance measured. Also, this resistance was investigated by letting weighted dead fish sink, head first, in a tank and by using optical arrangements for measuring their velocity.

In this period Breder in 'The locomotion of fishes' [3] published a review of fish swimming in which he gave names to a number of swimming forms of which we mention the following three: first, the anguiliform which is named after the swimming of the eel; second, the carangiform, where the front part of the body has little flexibility and the flexural movements are confined to the rear half or the rear one-third of the body length; third, the balistiform, where the propulsion is caused by the synchronized movements of dorsal and anal fins, while the body and the caudal fin are held rigid, by which the latter is of no direct use for the propulsion of the fish. For other forms of swimming we refer for instance to Blake in his book 'Fish locomotion' [4].

In the years around 1935 J. Gray studied the waves travelling posteriorly along the body of some fish such as the eel or the whiting. For this he used a machine for artificially imparting a wave motion to a flexible model or a dead fish. The famous paradox formulated by him about the power required for the propulsion of some fast swimming aquatic animals will be considered in Section 5.

As we already mentioned, the joint efforts of zoologists and engineers had been fruitful; however, yet a third group entered the scene in 1950 or thereabouts, namely the mathematically oriented scientists. These developed theories by which it became possible to make a quantitative analysis of swimming propulsion as a continuation of the previously developed qualitative theories.

Even the abstract mathematical theory of functional analysis seems to be useful for the third group. One reason is that it is of interest to optimize the swimming motion of a mathematical model of the fish, or part of it, with respect to its losses of kinetic energy into the fluid. Then, however, it has to be proved that, under certain suitable conditions, such an optimum motion does exist. This need not be the case, as we will demonstrate by rather simply formulated problems.

One of the early mathematically oriented investigators of the swimming of aquatic animals was G.I. Taylor, who published the article 'Analysis of the swimming of long and narrow animals' [5] in which he developed a so-called resistive theory. A bending wave travels with constant speed along the body of the animal. The forces per unit of length of each element of the swimming body are assumed to be the same as the resistance experienced per unit of length by a long cylinder with the same surface structure as that of the body and moving through the fluid with the same but now steady velocity and having the same inclination to the direction of the relative flow. This theory is suitable for the swimming of snakes, leeches and certain marine worms.

Later theories are often of a different type, for instance the reactive theory. In contrast with the mentioned resistive theory, this type of theory considers the flow of the fluid outside the thin boundary layer on the fish's body. By this the inertial effects of the fluid are dominant and an inviscid fluid model can be used.

After Lighthill's seminal paper 'Note on the swimming of slender fish' [6] and the fundamental paper of Wu 'Swimming of a waving plate' [7], many other mathematically oriented articles using reactive theories followed. This led to hydrodynamics getting a strong foothold in research on the swimming of fish.

In this paper we will consider reactive theories with an emphasis on basic principles of the swimming of fish and on the captivating early period when mathematically oriented studies were first published.

2. Some basic hydrodynamic concepts

It is of interest for the understanding of the swimming motion of fish to have insight in how momentum and energy are conveyed to an inviscid and incompressible fluid by a body with a time-dependent shape that moves in a fluid.

The fluid is assumed to be at rest at infinity with respect to a Cartesian coordinate system (x, y, z) (Figure 1). First we derive an expression for the change of the kinetic energy E of the fluid when a body B with boundary ∂B is moving through the fluid. The body is allowed to change its shape as well as its volume and can shed vorticity into the fluid. B is surrounded by a large control sphere H with radius R_H fixed in space. The region inside H, with the exception of B, is denoted by Ω.

Consider the equation of motion for an inviscid and incompressible fluid and the equation for the conservation of mass of the fluid

$$\rho \frac{\mathrm{d}\mathbf{v}}{\mathrm{d}t} = \rho \left\{ \frac{\partial \mathbf{v}}{\partial t} + (\mathbf{v} \cdot \text{ grad})\mathbf{v} \right\} = -\text{grad } p, \quad \text{div}\, \mathbf{v} = 0, \tag{2.1}$$

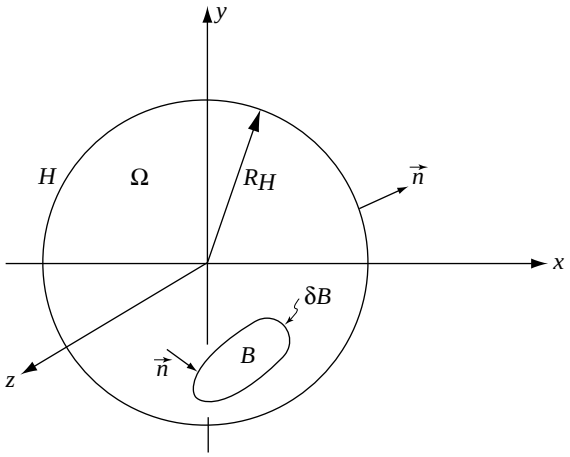

Figure 1. Deforming body B surrounded by large control sphere H.

where ρ is the density of the fluid, $\mathbf{v} = (v_x, v_y, v_z)$ its velocity and p the pressure.

It follows from (2.1) that

$$\rho \int_\Omega \mathbf{v} \cdot \left(\frac{\partial \mathbf{v}}{\partial t} + v_x \frac{\partial}{\partial x}\mathbf{v} + v_y \frac{\partial}{\partial y}\mathbf{v} + v_z \frac{\partial}{\partial z}\mathbf{v} \right) \mathrm{dVol} = -\int_\Omega \mathbf{v} \cdot \ \mathrm{grad}\ p \ \mathrm{dVol}. \tag{2.2}$$

Using $\mathrm{div}\,\mathbf{v} = 0$, we can write the left-hand side of (2.2) as

$$\tfrac{1}{2}\rho \int_\Omega \left\{ \frac{\partial}{\partial t}\mathbf{v}^2 + \ \mathrm{div}(\mathbf{v}^2 \cdot \mathbf{v}) \right\} \mathrm{dVol}. \tag{2.3}$$

The first part of this integral can be written as

$$\begin{aligned} \tfrac{1}{2}\rho \int_\Omega \frac{\partial}{\partial t}\mathbf{v}^2 \ \mathrm{dVol} &= \tfrac{1}{2}\rho \frac{\mathrm{d}}{\mathrm{d}t} \int_\Omega \mathbf{v}^2 \mathrm{dVol} - \tfrac{1}{2}\rho \int_{\partial B} \mathbf{v}^2 \cdot (\mathbf{v} \cdot \mathbf{n}) \ \mathrm{d}S_B = \\ &= \frac{\mathrm{d}\tilde{E}}{\mathrm{d}t} - \tfrac{1}{2}\rho \int_{\partial B} \mathbf{v}^2 \cdot (\mathbf{v} \cdot \mathbf{n}) \ \mathrm{d}S_B, \end{aligned} \tag{2.4}$$

where $\tilde{E}$ is the kinetic energy of the fluid in Ω and $\mathbf{n}$ is a unit normal on ∂B or on H, in both cases pointing out of Ω. The second part of (2.3) can be written as a surface integraL. Then, by using (2.4), we can reduce (2.3) to

$$\frac{\mathrm{d}\tilde{E}}{\mathrm{d}t} + \tfrac{1}{2}\rho \int_H \mathbf{v}^2 \cdot (\mathbf{v} \cdot \mathbf{n}) \ \mathrm{d}S_H. \tag{2.5}$$

The right-hand side of (2.2) can be brought into the form

$$-\int_\Omega \mathrm{div}(p \cdot \mathbf{v}) \ \mathrm{d\ Vol} = -\int_{\partial B} p \cdot (\mathbf{v} \cdot \mathbf{n}) \ \mathrm{d}S_B - \int_H p \cdot (\mathbf{v} \cdot \mathbf{n}) \ \mathrm{d}S_H. \tag{2.6}$$

It is easily seen that the integration over H tends to zero for $R_H \to \infty$. Then, by (2.5) and (2.6), we find by (2.2) for the rate of change of the kinetic energy E in the fluid

$$\frac{\mathrm{d}E}{\mathrm{d}t} = -\int_{\partial B} p \cdot (\mathbf{v} \cdot \mathbf{n}) \ \mathrm{d}S_B, \tag{2.7}$$

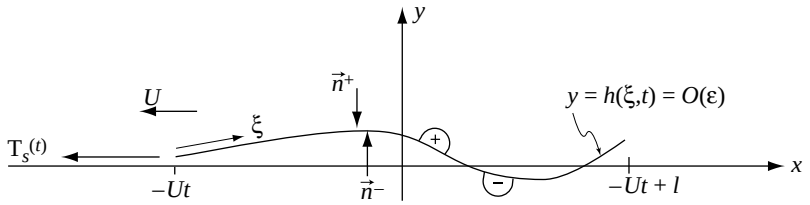

Figure 2. Two-dimensional swimming profile of zero-thickness, moving with velocity U in negative x-direction, suction force $T_s(t)$ at leading edge, length coordinate ξ with $0 \leq \xi < l$.

which states that the work carried out by the body on the fluid is transformed into kinetic energy of the fluid.

The kinetic energy that is thus transmitted to the fluid need not be lost but can be recovered completely or partly by succeeding motions of B. A complete recovery is easiest when no vorticity is shed into the fluid. For the sake of simplicity, consider a sphere without material mass of itself that is accelerated in the fluid by a constant force K in a fixed direction from rest to a velocity $V(t)$, without shedding vorticity. Then it has 'around it' kinetic energy E of the fluid which is proportional to V^2 and which can be written as $E = \frac{1}{2}\tilde{m}V^2$, where clearly such a constant $\tilde{m}$ must exist. This is called the virtual mass of the sphere. From conservation of energy we have the following relations

$$\frac{\mathrm{d}E}{\mathrm{d}t} = \tilde{m}V\frac{\mathrm{d}V}{\mathrm{d}t} = KV \rightarrow K = \frac{\mathrm{d}}{\mathrm{d}t}(\tilde{m}V), \tag{2.8}$$

which means that $(\tilde{m}V)$ is the momentum of the fluid 'around the body' in the direction of the motion.

Then by bringing the body to rest ($V = 0$) again by means of a decelerating force, the kinetic energy of the fluid is brought to zero and is recovered by the decelerating force.

Unfortunately, however, by extracting kinetic energy from the fluid by muscular motions of a fish, this energy cannot be used again completely by the fish. The reason is that, as biologists have shown, muscles have a positive energy cost, also when they do negative work. See also the second paragraph of Section 14.

In the case of a two-dimensional linear theory for a swimming profile (Figure 2), the energy relation (2.7) can also be used, but now per unit of length in the z-direction which is perpendicular to the (x, y) plane. Then, when the thickness of the profile tends to zero, the flow around the nose develops negative pressures which tend to $-\infty$, while the 'area of the nose' tends to zero. When the limit is taken, this causes a suction force $T_s(t)$ per unit of length acting at the nose in the direction of swimming.

The profile of thickness zero and length l swims with velocity U in the negative x-direction and remains in the neighbourhood of the x-axis in the case of a linear theory. Along the profile there is a length coordinate ξ which varies from $\xi = 0$ at the leading edge to l at the trailing edge of the profile. The time-dependent shape is $y = h(\xi, t) = O(\epsilon)$, where ϵ is a small parameter ($\epsilon/l \ll 1$). It can be proved that the suction force $T_s(t) = O(\epsilon^2)$. Within the accuracy of the linear theory the vorticity at the profile and the vorticity in the wake are at the x-axis.

We find from (2.7)

$$\frac{\mathrm{d}E(t)}{\mathrm{d}t} = \int_0^l [p(\xi, t)]_-^+ \left(\frac{\partial}{\partial t} + U\frac{\partial}{\partial \xi}\right) h(\xi, t)\,\mathrm{d}\xi - UT_s(t) = O(\epsilon^2), \tag{2.9}$$

where $[p(\xi,t)]_-^+ = p^+(\xi,t) - p^-(\xi,t) = O(\epsilon)$ is the pressure jump over the profile which, by the Kutta condition, has to be zero at the trailing edge $\xi = l$, so as to have a smooth flow at the trailing edge. When the pressure jump $[p]_-^+$ in the neighbourhood of the nose of the profile behaves as $\rho U Q(t)/\xi^{1/2}$ for $\xi \to 0$, then the suction force, reckoned positive in the negative x-direction, has the value

$$T_s(t) = \rho\frac{\pi}{4}Q^2(t) = O(\epsilon^2). \tag{2.10}$$

The power $P(t)$ needed for maintaining the swimming motion is

$$P(t) = \int_0^l [p(\xi,t)]_-^+\frac{\partial h}{\partial t}(\xi,t)\,\mathrm{d}\xi = -\int_0^l f(\xi,t)\frac{\partial h}{\partial t}(\xi,t)\,\mathrm{d}\xi = O(\epsilon^2), \tag{2.11}$$

where $f(\xi,t) = -[p(\xi,t)]_-^+$ are the external forces per unit of length, reckoned positive in the positive y-direction, needed to let the profile (which has neither bending stiffness nor inertia) execute its motion $h(\xi,t)$. In fact, these forces can replace the profile when they are placed on the right-hand side of the linearized version of the equation of motion (2.1).

The thrust $T(t)$ per unit of length brought about by the profile, reckoned positive in the negative x-direction, is

$$T(t) = -\int_0^l [p,(\xi,t)]_-^+\frac{\partial h}{\partial \xi}(\xi,t)\,\mathrm{d}\xi + T_s(t) = O(\epsilon^2). \tag{2.12}$$

Hence we find from (2.9), (2.11) and (2.12)

$$\frac{\mathrm{d}E(t)}{\mathrm{d}t} = P(t) - UT(t), \tag{2.13}$$

which shows that the power $P(t)$, needed to move the profile, minus the useful work/second, $UT(t)$, carried out by the profile, equals the rate of change of the kinetic energy in the fluid. This increase of energy does not need to remain in the fluid; it can be drained partly by the motion $h(\xi,t)$ of the profile at later moments. When, however, we consider a periodic motion of the profile with time period τ and when the mean shed energy is $\overline{E}$ per unit of time with

$$\overline{E} = \frac{1}{\tau}\int_0^\tau \frac{\mathrm{d}}{\mathrm{d}t}E(t)\,\mathrm{d}t \neq 0, \tag{2.14}$$

then $\overline{E}$ is lost per unit of time. This kinetic energy is left behind and equals the mean kinetic energy of the fluid induced by the shed vorticity over a length U far behind the profile.

The hydrodynamic efficiency η of the propulsion is defined by

$$\eta = \frac{U\overline{T}}{\overline{P}} = \frac{U\overline{T}}{U\overline{T} + \overline{E}}, \tag{2.15}$$

which is the mean useful power $U\overline{T}$ divided by the total mean power $\overline{P}$. In this linear theory, where $|\mathbf{v}|$, p and h are $O(\epsilon)$ and $\overline{T}_s = O(\epsilon^2)$, we have in general

$$\eta = 1 - O(\epsilon^0), \tag{2.16}$$

which does not tend to 1 for $\epsilon \to 0$.

Consider motions of the profile given by $\tilde{h}(\xi,t) = ch(\xi,t)$, where c is some constant. Then, the vorticity of the previous profile with motion $h(\xi,t)$ is multiplied by c and also its

slopes $\partial h(\xi, t)/\partial \xi$. The mean value of the thrust is multiplied by c^2. Hence the mean value of the lost kinetic energy, which depends on $\mathbf{v}^2$, is also multiplied by c^2. It follows that, in the linearized theory, the efficiency η (2.15) is the same as the efficiency of the original motion $h(\xi, t)$.

Finally we mention the case of small-amplitude swimming propulsion by two profiles, the first one swimming in front of the second one and both in an ϵ neighbourhood of the x-axis. Then the second profile can theoretically extract most of the kinetic energy (of $O(\epsilon^2)$) left behind per second by the first one by "approximately annihilating" the vorticity shed by the first one. The kinetic energy can be absorbed, so that only energy of $O(\epsilon^3)$ is left behind per second downstream of the trailing edge of the second profile. By this the efficiency of the cooperating two profiles, which in fact form one slotted profile, can be increased and becomes instead of (2.16)

$$\eta = 1 - O(\epsilon). \tag{2.17}$$

When ϵ is sufficiently small, (2.17) is more favourable than (2.16). For more information about (2.17) we refer to 'Hydrodynamic propulsion and its optimization' [8, pp. 166, 167, 201, 202] by J.A. Sparenberg.

This phenomenon can possibly be of interest for the interaction of the caudal fin of a fish with vorticity shed by its dorsal fin. However, we will discuss such interactions in Sections 7 and 10 where the points of view of Lighthill and Wu are given.

3. On the non-existence of optimum swimming motions and on efficiency-increasing travelling body waves

It is of interest to try to find algorithms for calculating optimum swimming motions with a high efficiency η (2.15). Then, for a desired mean thrust, the mean lost kinetic energy per unit of time has to be as small as possible. However, such an algorithm can be found only when an optimum motion does exist.

For a proof of the existence of optimum motions it seems that the abstract mathematical methods of functional analysis are unavoidable. One must then consider the kinetic energy lost per unit of time as a functional on a space of admitted motions. The functional and the space of motions should each possess properties ensuring that the functional assumes its minimum on at least one of the admitted motions. In Section 12 we return to this subject.

The opposite, however, namely the case when optimum motions do not exist, is also of interest. Then one is led to believe that extra constraints have to be put on the admitted motions so that an optimum motion exists and an algorithm can do its work to find such a motion.

When there does not exist an optimum motion, this does not mean that there are no motions which have a high efficiency within the framework of the considered theory. On the contrary, a non-existence proof can be based on the construction of a minimizing series of motions for which the loss of kinetic energy tends to zero, while the demanded thrust is still delivered. A general line of thought for a non-existence proof holding for any type of propulsion, either two- or three-dimensional, linear or nonlinear, is as follows.

(i) Assume it is possible to prove that, for any periodic motion F, for instance in the two-dimensional case $y = h(x, t)$, which satisfies the demanded constraints on its shape and delivers the desired mean thrust (per unit of length) $\overline{T} > 0$, there exists a $B > 0$ such that the lost mean kinetic energy/sec $\overline{E} = B$, where B depends on the considered motion.

(ii) Assume that it is possible to construct a minimizing series of motions F_n, for instance in the two-dimensional case $y = h_n(x,t), n = 1, 2, \ldots$, which satisfy the constraints on their shapes and deliver the mean thrust $\overline{T}$ for which the mean kinetic energy losses are $\overline{E}_n = B_n$ with $B_n \to 0$ for $n \to \infty$.

(iii) Then it follows that there does not exist an optimum motion F^* satisfying the constraints on its shape and yielding the desired mean thrust $\overline{T}$. The reason is that, if such a F^* existed it has by (i) lost kinetic energy per unit of time $\overline{E}^* = B^* > 0$. However, then we can find by (ii) a F_n with $0 < B_n < B^*$ which has lower kinetic energy losses than F^*, so F^* is not the optimum motion and hence there does not exist an optimum motion.

As an example of a non-existence proof of an optimum motion, we discuss the two-dimensional linear theory of a swimming profile without constraints on its motion. This example uses a method that shows how the thrust of a swimming profile can be favourably increased by superimposing on its motion travelling waves with a velocity equal to the swimming velocity. In a certain sense these waves occur also for the three-dimensional swimming motions of fish; however, there the velocity of the travelling wave is somewhat higher than the swimming velocity of the fish; see Section 5 point (5) and Section 6 below (6.22).

The flexible profile of length l is in the neighbourhood of the x-axis, its nose is at $x = 0$ while the fluid comes in with a velocity U in the positive x-direction. The profile has to deliver a mean thrust $\overline{T} > 0$ in the negative x-direction at the expense of a minimum energy loss. When the meaning is clear, the additions per unit of length or per unit of time are often suppressed.

That condition (i) is satisfied in the linear theory, when there is no slot in the profile, is discussed in [8, p. 307 and further]. This holds in the linear theory when there is no slot in the profile.

Now consider the lateral motion $y = a_1 h(x,t)$ where a_1 is a parameter. This motion is such that it induces, for instance, the following pressure jump $[p]^+_-$ over the profile.

$$[p]^+_- = a_1^2 \left(\sin \pi \frac{x}{l} \sin \pi \frac{U}{l} t \right), \quad 0 \leqslant x \leqslant l. \tag{3.1}$$

The shape $y = a_1 h_1(x,t)$ can be calculated and assumed to be known. Then at the $+$ side of the profile (Figure 2) we have a positive pressure for $nl/U < t < (n+1)l/U, n = 0, 2, 4, \ldots$, and a negative pressure for $n = 1, 3, 5, \ldots$. At the $-$ side the pressures are opposite for these time intervals.

On this motion we superimpose a travelling wave $y = a_2 h_2(x - Ut)$ of which a possible shape is drawn in Figure 3; it has a vertical part of height a_2. The wave may also have more smoothly varying values of y, but that complicates the reasoning. The vertical part translates with a velocity U in the positive x-direction and by leaving the profile at $x = l$, starts a new at $x = 0$, but is then reversed. It translates as in Figure 3a when the pressure is positive at the $+$ side of the profile and as in Figure 3b when the pressure is negative at the $+$ side. Thus, it introduces an extra thrust in the negative x-direction.

The mean kinetic energy $\overline{E}(a_1)$ left behind by the motion $y = a_1 h_1(x,t)$ can be written as

$$\overline{E}(a_1) = a_1^2 \overline{E}(a_1 = 1), \tag{3.2}$$

where $\overline{E}(a_1 = 1) > 0$ has some value that can be calculated. This lost energy is not changed by adding the motion of the travelling wave $y = a_2 h_2(x - Ut)$ moving with the velocity U and thus does not induce any velocity or vorticity in the fluid within the realm of the linear theory.

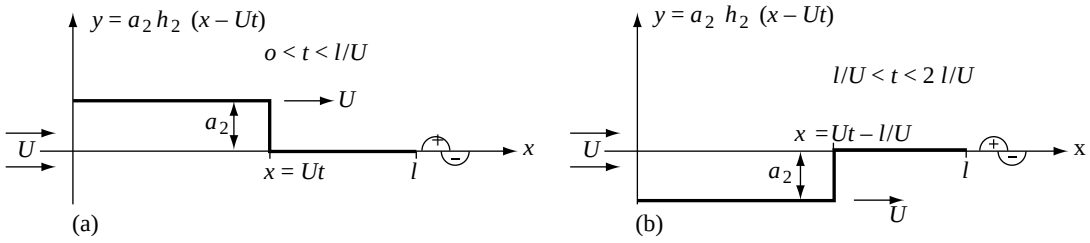

Figure 3. Shapes of wave $y = a_2h_2(x - Ut)$, (a) with $[p]^+_- > 0$, (b) with $[p]^+_- < 0$.

The mean thrust of the original motion $y = a_1h_1(x, t)$ can be written as

$$\overline{T}_1(a_1) = a_1^2\overline{T}_1(a_1 = 1), \tag{3.3}$$

where $\overline{T}_1(a_1 = 1)$ can turn out to be either positive or negative which is not important in what follows. The wave $y = a_2h_2(x-Ut)$ produces an extra mean thrust in the negative x-direction

$$\overline{T}_2(a_1, a_2) = a_2\left\{a_1^2\frac{U}{l}\int_0^{l/U} \sin^2 \pi\frac{U}{l}t \, \mathrm{d}t\right\} = \frac{1}{2\pi}a_1^2a_2, \tag{3.4}$$

because the force perceived by $y = a_2h_2(x - Ut)$ is proportional to the height a_2 of the step and to the pressure jump (3.1) at $x = Ut$ for $0 \leqslant t \leqslant l/U$. Then, a_1 and a_2 have to be chosen so that $\overline{T}_1(a_1) + \overline{T}_2(a_1, a_2) = \overline{T}$, which is the desired mean thrust reckoned positive in the negative x-direction. Hence, the efficiency (2.15) becomes

$$\eta(a_1, a_2) = \frac{U\{\overline{T}_1(a_1 = 1) + a_2/2\pi\}}{U\{\overline{T}_1(a_1 = 1) + a_2/2\pi\} + \overline{E}(a_1 = 1)}. \tag{3.5}$$

When $a_1 \to 0$ and a_2 increases as

$$a_2(a_1) = \frac{2\pi\{\overline{T} - a_1^2\overline{T}_1(a_1 = 1)\}}{a_1^2} \xrightarrow{a_1\to 0} \infty, \tag{3.6}$$

the total thrust remains equal to $\overline{T}$, while

$$\lim_{a_1\to 0} \eta(a_1, a_2) = 1. \tag{3.7}$$

We have now found a minimizing series of profile motions for $a_1 \to 0$ and $a_2 \to \infty$. It follows from the general considerations (i), (ii) and (iii) that there does not exist an optimum swimming motion in this linear two-dimensional theory when there are no constraints on the shapes. It is seen that the amplitude of the motions of the minimizing series increases unboundedly for $a_1 \to 0$ because $a_2 \to \infty$.

One might object that a linear theory is not valid then; this objection is correct. However, a linear theory has not an intrinsic value for the amplitude above which the theory may not be used and therefore a mathematical optimum motion cannot be found without further explicit constraints on the shapes of the admitted motions.

Also, it can be shown [8] that, even under the constraint $|h(x_1t)| < \delta$, where δ is a given number, there need not be an optimum motion. A minimizing series can also be found by considering profiles $y = a_1h_1(x, t; n)$ that induce pressure distributions with, instead of (3.1), a pressure jump $[p_n]^+_-$ of the form

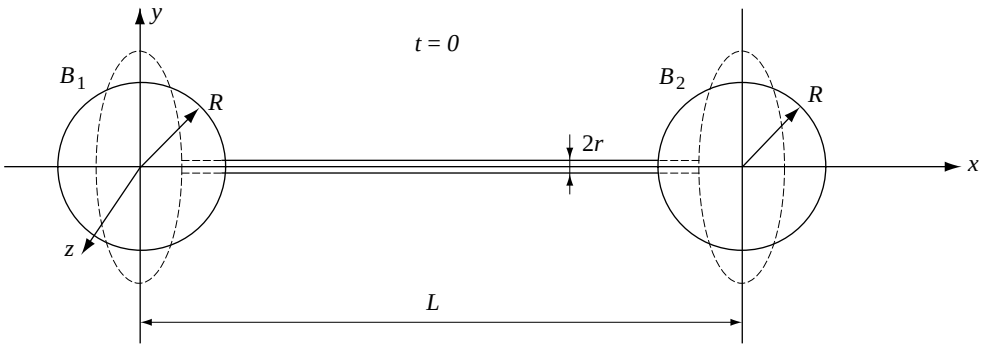

Figure 4. Body consisting of two 'deformable spheres', connected by narrow tube.

$$[p_n]_-^+ = a_1^2(-1)^n \sin \pi n \frac{x}{l} \sin \pi n \frac{U}{l} t, \quad n = 1, 2, \ldots . \tag{3.8}$$

Adequate shapes of superimposed travelling waves, say $y = a_2 h_2(x - Ut; n)$, can also be used to construct a minimizing series of swimming motions which lose their meaning for $n \to \infty$. In that case the amplitudes of the motions remain smaller than δ, but their wavelengths become shorter and shorter, whence these shapes do not tend to a usable motion.

This tending to a non-usable motion of the minimizing series of swimming motions is a general aspect of the non-existence of an optimum motion; see, for instance, [8] where some non-existence proofs are discussed.

4. Self-displacement of a deformable body in a perfect fluid without shedding vorticity

Consider a Cartesian coordinate system (x, y, z) embedded in an inviscid and incompressible fluid which is at rest with respect to the (inertial) coordinate system. A deformable body is in this fluid and is at rest. Then the question arises: is it possible that the body moves itself to another place by appropriate deformations, comes to rest there and has again its original shape and orientation while no vorticity is shed into the fluid? The fluid is then again at rest with respect to the (x, y, z) system. This movement elucidates elegantly the important idea of virtual mass.

P.G. Saffman showed in his article 'The self propulsion of a deformable body in a perfect fluid' [9] in a rather general way that this is possible. Here we discuss a simple example from which the principle becomes clear. It holds analogously for more realistic-looking bodies.

In the position at rest the 'animal' consists of two spheres B_1 and B_2 of radius R (Figure 4), the centres of which are at the x-axis and at a sufficiently large distance $L \gg R$ apart, so that their hydrodynamical interaction can be neglected. The spheres are connected by a very narrow tube of negligible mass the cross-section of which has radius $r \ll R$. This tube can lengthen and shorten itself and can thus exert forces K or $-K$ with a fixed value of K on the body parts at it ends or, when necessary, can lengthen or shorten itself without any force action by just following the body parts.

Each sphere $B_i (i = 1, 2)$ can change its shape into a flat axisymmetric ellipsoid, also denoted by B_i (dashed lines in Figure 4), while preserving its volume and centre. The circular midplane of such an ellipsoid is perpendicular to the x-axis. When m is the total mass (mechanical mass plus virtual mass) of the sphere of radius R, we can, by choosing an appropriate flatness of the ellipsoid, make the total mass $\tilde{m}$ of the ellipsoid equal to $\tilde{m} = km$ for any chosen

value $k > 1$. In the following an index $i (i = 1 \text{ or } 2)$ attached to a quantity means that the quantity belongs to B_i. So the total mass m_i of B_i can have the values $m_i = m$ or $m_i = km$, where from now on k has a chosen fixed value.

When x_i is the x-coordinate of the centre of B_i, $u_i = \mathrm{d}x_i/\mathrm{d}t$, τ is an interval of time and K_i is a force action on B_i in the positive x-direction, then we have for $0 \leqslant t \leqslant \tau$,

$$m_i \frac{\mathrm{d}^2 x_i(t)}{\mathrm{d}t^2} = K_i, \quad u_i(\tau) = \frac{K_i}{m_i}\tau + u_i(0), \quad x_i(\tau) = \tfrac{1}{2}\frac{K_i}{m_i}\tau^2 + u_i(0)\tau + x_i(0). \tag{4.1}$$

We can distinguish the following steps:

(1) We start the process at $t = 0$ from rest with $x_1(0) = 0, u_1(0) = 0, x_2(0) = L, u_2(0) = 0$ and consider $0 \leqslant t \leqslant \tau$ while

$$m_i = km, \quad K_1 = -K, \quad m_2 = m, \quad K_2 = K. \tag{4.2}$$

Then, analogous to (4.1), for $t = \tau$:

$$u_1(\tau) = -\frac{K}{km}\tau, \quad x_1(\tau) = -\tfrac{1}{2}\frac{K}{km}\tau^2, \quad u_2(\tau) = \frac{K}{m}\tau, \quad x_2(\tau) = \tfrac{1}{2}\frac{K}{m}\tau^2 + L. \tag{4.3}$$

(2) Take $m_1 = km$, $K_1 = 0$, $m_2 = m$, $K_2 = 0$, $\tau \leqslant t \leqslant 2\tau$; then u_1 and u_2 do not change and we find for $t = 2\tau$:

$$x_1(2\tau) = -\frac{3}{2}\frac{K}{km}\tau^2, \quad x_2(2\tau) = L + \frac{3}{2}\frac{K}{m}\tau^2. \tag{4.4}$$

(3) Take $m_1 = km$, $K_1 = K$, $m_2 = m$, $K_2 = -K$, $2\tau \leqslant t \leqslant 3\tau$; then we find for $t = 3\tau$:

$$x_1(3\tau) = -2\frac{K}{km}\tau^2, \quad u_1(3\tau) = 0, \quad x_2(3\tau) = L + 2\frac{K}{m}\tau^2, \quad u_2(3\tau) = 0. \tag{4.5}$$

(4) Take $m_1 = m$, $K_1 = K$, $m_2 = km$, $K_2 = -K$, $3\tau \leqslant t \leqslant 4\tau$; then we find for $t = 4\tau$:

$$\begin{aligned} &x_1(4\tau) = \left(\frac{1}{2} - \frac{2}{k}\right)\frac{K}{m}\tau^2, \quad u_1(4\tau) = \frac{K}{m}\tau, \quad x_2(4\tau) = L + \left(2 - \frac{1}{2k}\right)\frac{K}{m}\tau^2, \\ &u_2(4\tau) = -\frac{K\tau}{km}. \end{aligned} \tag{4.6}$$

(5) Take $m_1 = m$, $K_1 = 0$, $m_2 = km$, $K_2 = 0$, $4\tau \leqslant t \leqslant 5\tau$; then u_1 and u_2 do not change and we find for $t = 5\tau$:

$$x_1(5\tau) = \left(\frac{3}{2} - \frac{2}{k}\right)\frac{K}{m}\tau^2, \quad x_2(5\tau) = L + \left(2 - \frac{3}{2k}\right)\frac{K}{m}\tau^2. \tag{4.7}$$

(6) Take $m_1 = m$, $K_1 = -K$, $m_2 = km$, $K_2 = K$, $5\tau \leqslant t \leqslant 6\tau$; then we find for $t = 6\tau$:

$$\begin{aligned} &x_1(6\tau) = 2\left(1 - \frac{1}{k}\right)\frac{K}{m}\tau^2, \quad u_1(6\tau) = 0, \quad x_2(6\tau) = L + 2\left(1 - \frac{1}{k}\right)\frac{K}{m}\tau^2, \\ &u_2(6\tau) = 0. \end{aligned} \tag{4.8}$$

Now let B_2 assume its original spherical shape. Then we have the starting configuration again since $u_1(6\tau) = u_2(6\tau) = 0$ and the distance between B_1 and B_2 is again L. However, because $k > 1$, the centres of B_1 and B_2 have moved along the x-axis over a distance $2(1 - k^{-1})K\tau^2/m > 0$.

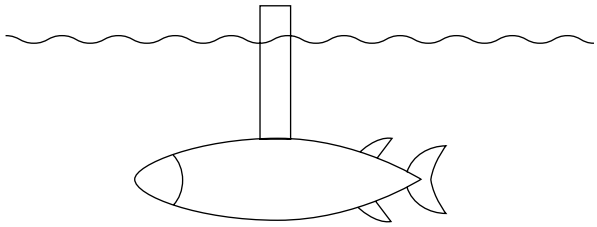

Figure 5. Robotic model of a swimming blue fin tuna. From Barret *et al*. [12]

After this we can repeat the process by which the deformable body can move over arbitrarily large distances along the x-axis without shedding vorticity, starting from rest and coming to rest again.

It is shown in [8, p. 63] that a body of finite extent, moving periodically through an inviscid and incompressible fluid without shedding vorticity, cannot exert a force with a non-zero mean value. This means that the swimming creature we just considered cannot develop a non-zero mean thrust in its idealized environment.

5. Increase or decrease of drag by the body movements of swimming fish

There is a famous paradox formulated by J. Gray in his article 'Studies in animal locomotion VI. The propulsion powers of the dolphin' [10]. Gray estimated among other things the power needed for a dolphin of length 1·82 m to swim at a speed of 10·1 m/s. This he did by calculating the dolphin's resistance by means of a drag coefficient based on a turbulent boundary layer. He found that the required power was possibly about seven times the estimated muscular power available for propulsion. This yields the paradox which is considered by a large number of investigators.

The paradox is, however, rather difficult to tackle because of the lack of a common opinion among investigators on the influence of the swimming motion on the resistance of the body. Some opinions are that the resistance of the swimming body can be increased by a factor of three with respect to the resistance of the body when it glides motionless through the water; see for instance M.J. Lighthill's 'Large-amplitude elongated-body theory of fish locomotion' [11].

In order to give some information about the latter problem we discuss the experimental article of D.S. Barret *et al.*, 'Drag reduction in fish-like locomotion', [12]. An experiment is carried out by means of a robotic mechanism which has the shape of a blue-fin tuna of which we give a short description.

The model has a caudal, a dorsal and a ventral fin; Figure 5. Its length $L = 1{\cdot}25$ m; the maximum lateral dimensions at midlength are height 0·3 m and width 0·21 m. The lunate tail has a vertical span of 0·32 m.

The model consists of eight rigid links, the last one being the caudal fin. The links can rotate with respect to their neighbouring links and are controled by strings moving over pulleys and activated by a number of motors. The second link is fixed to a streamlined strut, which itself is fixed to an overhead carriage. The first link and the third one are coupled so as to move in antiphase. The links are covered by a skin structure that consists of layers of filter foam and thin latex sheets.

The lateral motion of the 'spinal column' of the model has the shape

$$y(x, t) = (C_1 x + C_2 x^2)\ \sin(kx - \omega t), \tag{5.1}$$

where C_1, C_2, k and ω are parameters and x is measured from the edge of the second link.

An important dimensionless quantity is the Strouhal number St

$$\mathrm{St} = fA/U, \tag{5.2}$$

where f is the frequency of the oscillation, A the double amplitude of the tail at its junction to the body and U is the swimming speed.

Drag reduction is said to occur when the net power supplied by the motors needed for self-propulsion is less than the power needed to tow the body in stretched form with the same speed.

In all experiments the swimming speed is $U = 0{\cdot}7$ m/sec, the Reynolds number $Ul/\nu \approx 10^6$ and the Strouhal number is $\mathrm{St} = 0{\cdot}16$. The following ranges of important quantities were examined:

(1) Phase angle at the tail between lateral and angular motion, $80^\circ \leqslant \psi \leqslant 100^\circ$.

(2) Body wavelength, $1\ \mathrm{m} \leqslant \lambda = 2\pi/k \leqslant 1{\cdot}5$ m.

(3) Nominal angle of attack of tail, $15^\circ \leq \alpha \leq 25^\circ$.

(4) Double amplitude A; drag reduction is not very sensitive to A for $A > 0{\cdot}13$ m.

(5) Drag reduction occurred only when the phase speed of the travelling wave in the body was larger than the swimming speed U.

For self-propelled motions maximum drag reductions of around, 50% were found, while for extra thrust-producing motions drag reductions exceeding 70% were realized in some cases. This latter drag reduction is perhaps of interest for the burst-and-glide swimming of fish where extra thrust is needed for the acceleration phase of this type of swimming; see Section 15 of this survey.

As possible reasons for drag reduction are mentioned in [12]:

(i) Laminarization of the boundary layer by the motion of the body.

(ii) Favourable interaction of the vorticity shed by the tail with that by the body, the dorsal and the ventral fins.

It should be remarked that, in spite of the care that has been exercised in doing the measurements reported in the paper under consideration, not all investigators are convinced that drag reduction was indeed demonstrated. Hence, further experiments seem to be needed to arrive at a common opinion about the very interesting influence of the swimming motion of a fish on its drag. However, other mechanisms, such as the drag-reducing mucus or fish slime, the induction and the maintenance of an appropriate turbulent boundary layer and a viscous or dynamic damping capacity of the skin, have to be considered also [4].

6. On the swimming of slender fish

The already mentioned seminal article 'Note on the swimming of slender fish' [6], written by Lighthill, appeared in 1960 and was a break-through in the mathematically oriented research on the swimming of fish. It discusses a reactive theory where the forces on the moving body of the fish are caused by the inertia of the water set into motion.

Lighthill's slender-body theory uses a small parameter ϵ so that, when l is the length of the body and U its swimming velocity, the lateral dimensions of the body are $0(\epsilon l)$ and the induced velocities are $0(\epsilon U)$, while these quantities change sufficiently gradually along the

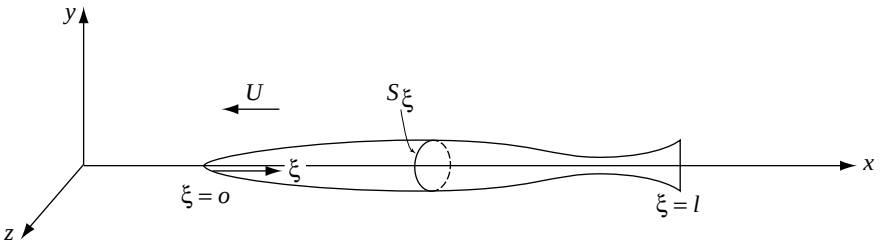

Figure 6. Slender fish swimming with velocity U in the negative x-direction, in the neighbourhood of the x-axis.

body. Then, roughly spoken, quantities in an equation which are of the lowest order in ϵ are used, while quantities of a higher order are neglected.

First we discuss the more or less heuristic method that Lighthill presents in the first part of his paper. An outline of the fish is drawn in Figure 6 as it swims with velocity U in the negative x-direction. Along the fish we have a length parameter ξ with $\xi = 0$ at the nose of the fish and $\xi = l$ at the trailing edge of its tail. In the first instance we assume that the fish has only a caudal fin with a vertical trailing edge; hence it has no dorsal or ventral fins.

During the swimming the cross-sections S_ξ of the body will be moved in the z-direction over a distance $h(\xi, t) = 0(\epsilon)$ without changing their shape.

Then, by the slenderness of the body, the fluid flow at ξ is nearly two-dimensional in the neighbourhood of the body. We obtain an approximation of the flow by considering the flow induced by a two-sided infinitely long cylinder C_ξ with cross-section S_ξ translating through the fluid in the z-direction with the velocity

$$V(\xi, t) = \frac{\partial h}{\partial t}(\xi, t) + U\frac{\partial h}{\partial \xi}(\xi, t). \tag{6.1}$$

The first term at the right-hand side of (6.1) is the lateral velocity of the cross-section S_ξ and the second term expresses that the body of the fish is struck by the fluid at an angle $\partial h(\xi, t)/\partial \xi$.

Per unit of length the cylinder C_ξ has around it an amount of momentum in the z-direction of magnitude (2.8), *viz.*

$$m(\xi)V(\xi, t), \tag{6.2}$$

where $m(\xi)$ is the virtual mass belonging to the cross-section S_ξ.

Thus, the instantaneous force L in the z-direction per unit of length exerted by the fluid on the body becomes (2.8):

$$L(\xi, t) = -\frac{\mathrm{d}}{\mathrm{d}t}\{V(\xi, t)m(\xi)\} = -\left(\frac{\partial}{\partial t} + U\frac{\partial}{\partial \xi}\right)\{V(\xi, t)m(\xi)\}. \tag{6.3}$$

Using $L(\xi, t)$ we may calculate other quantities such as the mean power $\overline{P}$ that the fish has to perform during swimming. After some manipulations Lighthill finds

$$\overline{P} = -\overline{\int_0^l \frac{\partial h}{\partial t}(\xi, t)L(\xi, t)\,\mathrm{d}\xi} = Um(\xi)\left.\overline{\left[\frac{\partial h(\xi, t)}{\partial t}\left\{\frac{\partial h(\xi, t)}{\partial t} + U\frac{\partial h(\xi, t)}{\partial \xi}\right\}\right]}\right|_{\xi=l}, \tag{6.4}$$

where a bar stands for taking the mean value with respect to time.

In this theory the loss of kinetic energy into the fluid occurs at the trailing edge of the tail of the fish. Per unit of length, the amount of kinetic energy at the end of the tail is $\frac{1}{2}m(l)V^2(l,t)$. Because the fish swims with the velocity U, it follows that the rate of shedding kinetic energy into the fluid behind the tail becomes

$$\tfrac{1}{2}Um(l)V^2(l,t). \tag{6.5}$$

Then, by assuming that the conservation of energy analogous to (2.13) holds also in this theory, we find for the mean value of the thrust $\overline{T}$, after some reduction

$$\overline{T}U = \overline{P} - \tfrac{1}{2}Um(l)\overline{V^2(l,t)} = \tfrac{1}{2}Um(l)\left\{\overline{\left(\frac{\partial h}{\partial t}(\xi,t)\right)^2} - U^2\overline{\left(\frac{\partial h(\xi,t)}{\partial \xi}\right)^2}\right\}\Bigg|_{\xi=l}. \tag{6.6}$$

These more or less heuristic considerations, as Lighthill himself says, 'are attractively simple but may not be overwhelmingly convincing'. Therefore he also gives an analytical derivation of the above results, which then turn out to be correct.

We will give an impression of Lighthill's expert mathematical justification of the above results by discussing two of its salient points. Now we assume the undisturbed fluid to flow with a velocity U in the positive x-direction with respect to the (x, y, z) system, while the fish's nose stays in the neighbourhood of the origin. One of the difficulties of the theory is the formulation of the exact boundary conditions on the swimming body for the velocity field of the fluid. This we will discuss first.

The surface S of the body of the fish, when it is stretched and at rest, is in the neighbourhood of the x-axis for $0 \leq x \leq l$. In this stretched condition the surface of the body is denoted by:

$$F(x, y, z) = 0. \tag{6.7}$$

When the fish swims, its cross-sections S_x get the already mentioned lateral displacement $h(x,t)$ in the z-direction. In order to find the flow boundary conditions on the body, Lighthill introduces a new coordinate system (X, Y, Z) and a time $\tilde{T}$ which are related to the original ones by

$$X = x, \quad Y = y, \quad Z = z - h(x,t), \quad \tilde{T} = t. \tag{6.8}$$

Hence, there exist the relations $h(x,t) = h(X, \tilde{T})$ (same formulas) and

$$\frac{\partial}{\partial x} = \frac{\partial}{\partial X} - \frac{\partial h}{\partial x}\frac{\partial}{\partial Z}, \quad \frac{\partial}{\partial y} = \frac{\partial}{\partial Y}, \quad \frac{\partial}{\partial t} = \frac{\partial}{\partial \tilde{T}} - \frac{\partial h}{\partial t}\frac{\partial}{\partial Z},$$

$$\frac{\partial h}{\partial x}(x,t) = \frac{\partial}{\partial X}h(X,\tilde{T}), \quad \frac{\partial h}{\partial t}(x,t) = \frac{\partial}{\partial \tilde{T}}h(X,\tilde{T}). \tag{6.9}$$

In this new coordinate system the body of the fish, when it is swimming, is described by

$$F(X, Y, Z) = 0, \tag{6.10}$$

which is independent of the time $\tilde{T}$.

In the new coordinates the three-dimensional potential equation for the velocity potential becomes

$$\left(\frac{\partial}{\partial X}-\frac{\partial h}{\partial X}\frac{\partial}{\partial Z}\right)\left(\frac{\partial\varphi}{\partial X}-\frac{\partial h}{\partial X}\frac{\partial\varphi}{\partial Z}\right)+\frac{\partial^2\varphi}{\partial Y^2}+\frac{\partial^2\varphi}{\partial Z^2}=0, \tag{6.11}$$

where $\varphi=\varphi(X,Y,Z,\tilde{T})$. Because quantities change gradually in the x-direction, differentiations with respect to x are small in slender-body theory, whence (6.11) can be reduced to

$$\frac{\partial^2\varphi}{\partial Y^2}+\frac{\partial^2\varphi}{\partial Z^2}=0. \tag{6.12}$$

The boundary condition for the velocity potential becomes

$$\begin{aligned}&\frac{\mathrm{d}F}{\mathrm{d}t}(x,y,z-h(x,t))=\frac{\partial F}{\partial t}+\frac{\partial\varphi}{\partial x}\frac{\partial F}{\partial x}+\frac{\partial\varphi}{\partial y}\frac{\partial F}{\partial y}+\frac{\partial\varphi}{\partial z}\frac{\partial F}{\partial z}=\\&=-\frac{\partial h}{\partial\tilde{T}}\frac{\partial F}{\partial z}+\left(\frac{\partial\varphi}{\partial X}-\frac{\partial h}{\partial X}\frac{\partial\varphi}{\partial Z}\right)\left(\frac{\partial F}{\partial X}-\frac{\partial h}{\partial X}\frac{\partial F}{\partial Z}\right)+\frac{\partial\varphi}{\partial Y}\frac{\partial F}{\partial Y}+\frac{\partial\varphi}{\partial Z}\frac{\partial F}{\partial Z}=0,\end{aligned} \tag{6.13}$$

$$(X,Y,Z)\in F(X,Y,Z)=0,\quad\forall\tilde{T}. \tag{6.14}$$

After this key transformation, the slender-body theory is developed in a, be it complicated but, straightforward way by neglecting quantities that are relatively small. For this we refer to the paper under consideration [6].

However, in this exact theory, besides the transformation another craft is demonstrated by Lighthill that we like to describe. In order to find the thrust of the body in the X-direction, besides other integrals, the integral over the body surface S

$$T_2(\tilde{T})=\iint_S p_2\,\mathrm{d}Y\,\mathrm{d}Z, \tag{6.15}$$

has to be calculated, where p_2 is the pressure around the cylinder C_X with cross-section S_X which translates steadily through the fluid in the Z-direction with a constant velocity ${}^*V$ which is the value of $V(x,t)$ at the considered place and time. By an elegant reasoning Lighthill finds a remarkably simple expression for (6.15).

For this purpose (6.15) for a cross-section S_X at a fixed value of X and over a width δX is considered first. This integral can be written by using the notation of Figure 7 as

$$-\int_{S_X} p_2(s)\,\delta n(s)\,\mathrm{d}s, \tag{6.16}$$

where s is a length parameter along S_X. The kinetic energy of the fluid per unit of length of the cylinder C_X with cross section S_X is $\frac{1}{2}{}^*V^2m(X)$, where, as before, $m(X)$ is the virtual mass per unit of length of C_X.

If, during the translation with constant velocity ${}^*V$, the cylinder C_X undergoes gradually a small change of cross-section from S_X to $S_{X+\delta X}$, then the fluid momentum will change by the amount

$${}^*V\delta m(X)={}^*V\frac{\mathrm{d}m}{\mathrm{d}X}\delta X. \tag{6.17}$$

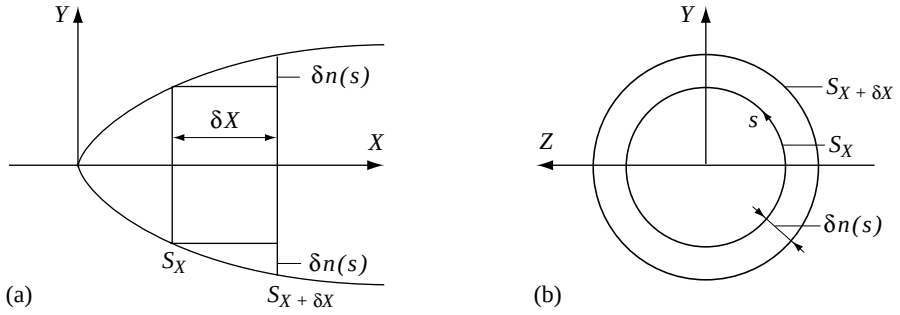

Figure 7. The cross sections S_X and $S_{X+\delta X}$, the length parameter s along S_X and $\delta n(s)$.

To bring about this change of momentum, the translating and expanding C_X must do work per unit of its length, which can be calculated as follows. Because ${}^*V$ is constant, the force in the direction of translation needed to change the momentum is $\mathrm{d}({}^*Vm)/\mathrm{d}t = {}^*V\ \mathrm{d}m/\mathrm{d}t$ and, hence, the power needed is ${}^*V^2\ \mathrm{d}m/\mathrm{d}t$. Thus, the work carried out by this force per unit of length of C_X, becomes

$$ {}^*V^2 \int \frac{\mathrm{d}m}{\mathrm{d}t}\mathrm{d}t = {}^*V^2 \delta m(X). \tag{6.18} $$

During this motion the outward-moving elements of area of the varying C_X also do work against the pressure p_2. Hence, per unit of length of C_X, the surface of C_X has to do an amount of work that can be written as minus the integral (6.16) that we want to calculate, because $\delta n(s)$ is in the direction of the increase of S_X towards $S_{X+\delta X}$.

The change of the kinetic energy is $\frac{1}{2}{}^*V^2\delta m(X)$, which has to be equal to the total work exerted on the fluid. Hence by (6.18) and (6.16)

$$ \frac{1}{2}{}^*V^2\delta m(X) = {}^*V^2\delta m(X) + \int_{S_X} p_2(s)\delta n(s)\ \mathrm{d}s \tag{6.19} $$

from which follows (6.16). Then, for (6.15) we still have to carry out an integration with respect to X,

$$ T_2(\tilde{T}) = \frac{1}{2}\int_0^l V^2(X,\tilde{T})\frac{\mathrm{d}m(X)}{\mathrm{d}X}\,\mathrm{d}X, \tag{6.20} $$

where now we have replaced ${}^*V$ by its time-dependent original $V(X,\tilde{T})$. So by this peculiar reasoning $T_2(\tilde{T})$ (6.15) can be determined without a knowledge of the special shape of $S_X(X)$; only its virtual mass is of importance.

Further Lighthill discusses the so-called recoil conditions. By (6.3) and (6.6) it is possible to calculate the forces acting on the body of the fish when its lateral motion $z = h(x,t)$ is prescribed. Then, it is clear that, by these forces on its body, the fish will move, when it is left free in space, in a way that is most probably different from this prescribed motion. However, the calculated forces are then incorrect, unless these forces satisfy the mentioned recoil conditions. These are:

(i) The resultant of the lateral forces exerted by the fluid on the body has to be equal to the rate of change of momentum in the z-direction of the body.

(ii) The resultant of the moment, for instance around the y-axis, of the lateral forces has to be equal to the rate of change of the angular momentum of the body around the y-axis.

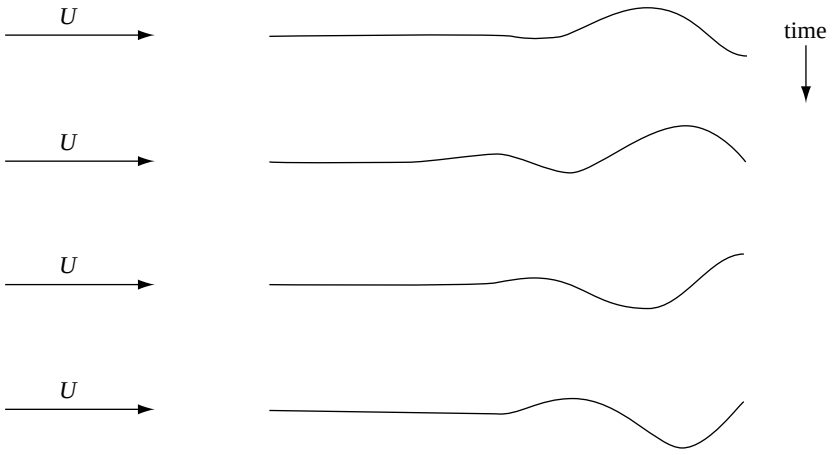

Figure 8. Swimming movements with good efficiency, suggested by Lighthill [6].

When $S(x)$ denotes the area of a cross-section S_x of the body and we assume that the density of the fish is approximately equal to the density ρ of water, these two conditions can be formulated as

$$\rho \int_0^l \begin{pmatrix} 1 \\ x \end{pmatrix} S(x) \frac{\partial^2 h}{\partial t^2} \mathrm{d}x = -\int_0^l \begin{pmatrix} 1 \\ x \end{pmatrix} \left(\frac{\partial}{\partial t} + U \frac{\partial}{\partial x} \right) \left\{ m(x) \left(\frac{\partial h}{\partial t} + U \frac{\partial h}{\partial x} \right) \right\} \mathrm{d}x, \quad \forall t, \tag{6.21}$$

where in $\binom{1}{x}$, 1 has to be taken for condition (i) and x for condition (ii).

With respect to the time-dependent thrust, an analogous recoil condition in the x-direction is not needed, because the mass of the fish is $O(\epsilon^2)$, while the time-dependent thrust is only $O(\epsilon^3)$.

In fact, the conditions (i) and (ii) put a constraint on the choice of $h(x,t)$ that is very difficult to be satisfied in advance. In general, those conditions are taken into account only approximately by an *a priori* inspection of $h(x,t)$; see below.

The hydrodynamic efficiency becomes

$$\eta = U\overline{T}/\overline{P}, \tag{6.22}$$

where $\overline{T}$ and $\overline{P}$ are given in (6.6) and (6.4), respectively. Lighthill argues that a good efficiency is obtained when a travelling wave $h(x,t) = g(x)\cos\,\omega(t - x/c)$ travels down the body of the fish with an amplitude $g(x)$ that increases towards the tail and a velocity c that is somewhat larger than the swimming velocity U. Possibly this has a relation with the idealized travelling wave introduced below (3.1) which increased the efficiency of the swimming motion there.

Combining several aspects, Lighthill arrives at the conclusion that the carangiform of swimming, that is with a rather stiff front part of the body and with the tail part having a positive and a negative phase, so that the moments (condition (ii)) produced by each of them tend to cancel out, will yield a good efficiency. He suggests a cycle of movements as shown in Figure 8.

This theory of Lighthill was extended by R. Coene in his 'Notes on the efficiency of propulsion of bodies in waves' [13], who applies some of the ideas of Lighthill, for instance the coordinate transformation (6.8), to a slender aquatic animal with a horizontal tail swimming under surface waves. The depth of swimming is such that the disturbance of the water surface

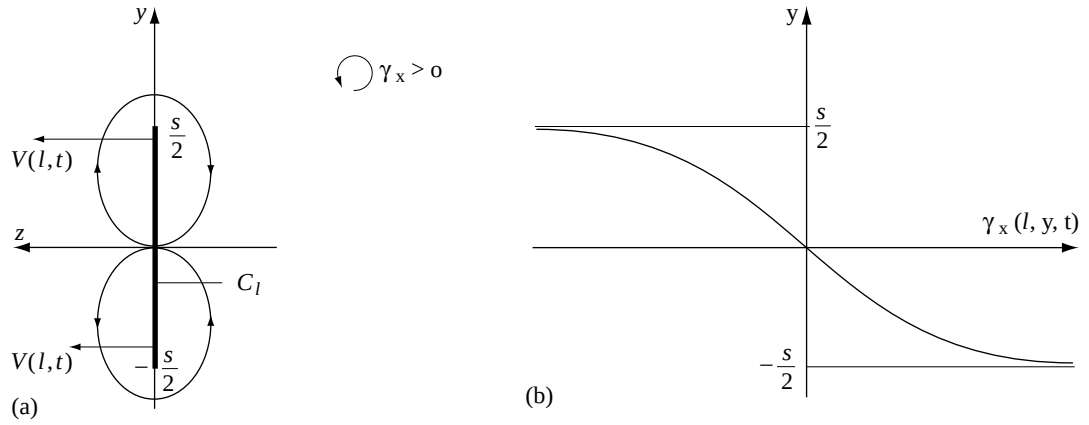

Figure 9. (a)Flow around strip C_l, $|y| \leq \frac{s}{2}$, $z = 0$; (b) strength of vorticity $\gamma_x(l, y, t)$ on strip C_l.

can be neglected; however, energy can be extracted from the velocity field induced by the waves whose crests are perpendicular to the direction of swimming.

7. On vorticity shedding by fins in slender-body theory

In his article 'Aquatic animal propulsion of high hydrodynamical efficiency' [14], Lighthill continues among other things the subject of the previous section by studying the vorticity shed by fins and its influence on the swimming of a slender fish.

The simplest case, which we already mentioned briefly, is when the fish has only a caudal fin of which the trailing edge is straight and vertical, $|y| \leq \frac{1}{2}s$; Figure 9a. Then, in slender-body theory the cylinder C_l introduced above (6.1) belonging to the trailing edge at $x = l$ (Figure 6) with the nose of the fish at the origin, is a two-sided infinitely long flat strip of width s. In order to find the two-dimensional approximation of the flow at the trailing edge, this strip has to be translated in a direction perpendicular to itself with the velocity

$$V(l,t) = \left\{ \frac{\partial h}{\partial t}(x,t) + U\frac{\partial h}{\partial x}(x,t) \right\}\Bigg|_{x=l}, \tag{7.1}$$

where $z = h(x,t)$ is again the lateral motion of the fish body. The two-dimensional flow and the vorticity component $\gamma_x(l, y, t)$ in the x-direction needed to prevent the fluid passing through C_l are drawn in Figures 9a and 9b, respectively, where

$$\gamma_x(l, y, t) = -2V(l,t)\frac{y}{(\frac{s^2}{4} - y^2)^{1/2}}, \quad |y| \leq \frac{s}{2}, \quad z = 0, \tag{7.2}$$

which belongs to an elliptic lift distribution along the trailing edge of the tail.

This vorticity is left behind when the fish moves on by swimming with the velocity U. It is clearly an approximation of the 'real' shed vorticity, caused by the character of the slender-body theory, namely there is no γ_y component which is needed to make the vorticity field free of divergence, because $V(l,t)$ changes with time.

Now we consider the influence of free vorticity shed by fins on downstream parts of the body of the swimming fish. First, we follow Lighthill's discussion of the vorticity shed by a dorsal fin with a straight trailing edge towards an other at a short downstream distance from

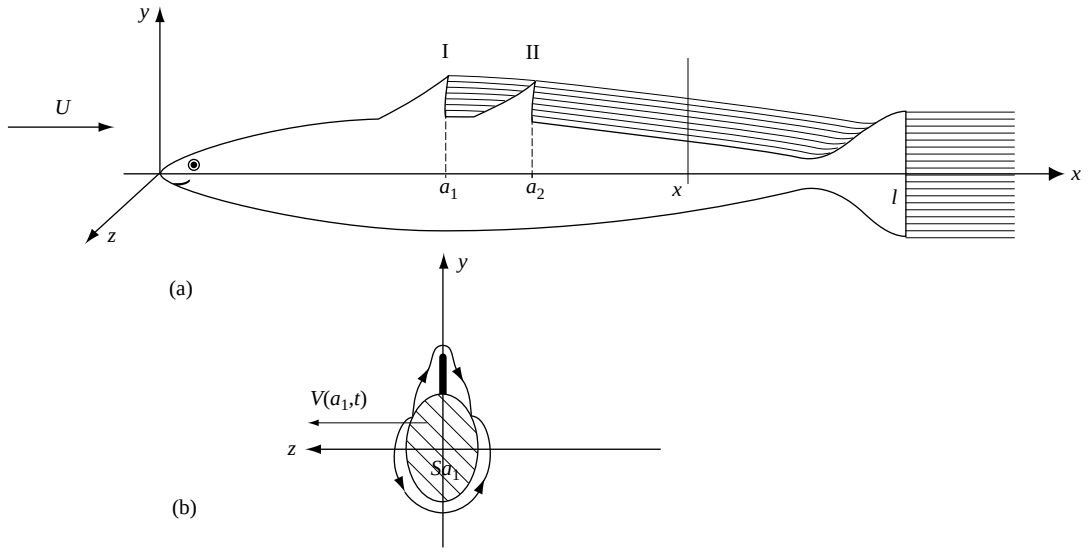

Figure 10. (a) Fish with two closely spaced dorsal fins I and II with vertical trailing edges; (b) two-dimensional flow around cylinder C_{a_1} which has the cross-section S_{a_1} of the body of the fish at $x = a_1$.

the first one; Figure 10a. The foremost fin I with trailing edge at $x = a_1$, sheds free vorticity analogously to the shedding of the vorticity by the caudal fin. Now, however, the lower part of the cylinder C_{a_1} has an oval shape and this causes the vorticity γ_x at the trailing edge of the protruding fin to be different from (7.2). Because the vorticity γ_x in the neighbourhood of the trailing edge of fin I induces there the velocity $V(a_1, t)$, it will continue to do so when it has left fin I and is in between fin I and fin II. In slender-body-theory changes in the x-direction are gradual, hence the velocity in the z-direction of the body at the place of the nearby fin II will not differ much from the lateral velocity of fin I. This means that the gap in between fin I and fin II, filled with the shed vorticity, behaves nearly as if fin I and fin II were connected by an intermediate material sheet. From this Lighthill concludes that closely spaced fins have nearly the same influence on the swimming as one continuous fin, but since the speed of the travelling body wave is somewhat larger than the swimming velocity, there is a slight phase difference between the motions of fin I and fin II.

Second, we consider the vorticity shed by fin II, which can travel over larger distances in the x-direction; hence we have to take into account that at place x, with x really larger then a_2, the momentary free vorticity at that location is shed by fin II at the previous time $(t - (x - a_2)/U)$ and will be proportional to

$$V\left(a_2, t - \frac{(x - a_2)}{U}\right). \tag{7.3}$$

The free vorticity $\gamma_x^{(1)}(x = a_2, y)$ as a function of y, for a transverse velocity in the z-direction of magnitude 1, can be calculated from the shape of the cross-section S_{a_2} of the cylinder C_{a_2}. This means that the free vorticity $\gamma_x(x, y, t)$ for $x > a_2$ at the dorsal side of the body becomes

$$\gamma_x(x, y, t) = V(a_2, t - \frac{(x - a_2)}{U}) \cdot \gamma^{(1)}(a_2, y), \tag{7.4}$$

where, for instance, it is assumed that this vorticity lies straight behind fin II.

It is not clear where Lighthill chose the shed vorticity with respect to the body of the fish. Does the vorticity remain in a flat strip straight behind fin II or does it in some sense follow the streamlines caused by the body? However, this is not important for the following analysis, as long as the free vorticity remains almost in the x, y plane. We return to this subject in the final paragraph of this section.

As before Lighthill denotes by $m(x)$ the virtual mass per unit of length in the z-direction of the cylinder C_x with cross-section S_x of the body of the fish in the absence of the shed vorticity (7.4). For the one-valued velocity potential $\varphi(x, y, z, t)$ of the two-dimensional flow induced by C_x there are the boundary conditions (7.1):

$$\frac{\partial \varphi}{\partial n} = V(x,t)n_z \quad \text{on} \quad C_x, \qquad \varphi = 0 \quad \text{on} \quad z = 0 \quad \text{outside} \quad C_x, \tag{7.5}$$

where n_z is the z-component of the unit normal on C_x and it is assumed that the fish at rest is symmetrical with respect to the plane $z = 0$.

The one-valued function $\tilde{\varphi}(x, y, z, t)$ denotes the velocity potential of the flow belonging to the known vortex sheet (7.4) and the cylinder C_x at rest. This two-dimensional flow satisfies the boundary conditions

$$\frac{\partial \tilde{\varphi}}{\partial n} = 0 \quad \text{on} \quad C_x \quad \text{and a known jump of } \tilde{\varphi} \text{ across the vortex sheet.} \tag{7.6}$$

By introducing $\tilde{m}(x)$ we can write the momentum of this flow in the z-direction as $\tilde{m}(x) \cdot V(a_2, t - (x - a_2)/U)$.

The velocity potential of the total flow induced by the transverse motion of C_x in the presence of the vortex sheet is $(\varphi + \tilde{\varphi})$ and its momentum in the z-direction becomes

$$m(x)V(x,t) + \tilde{m}(x)V\left(a_2, t - \frac{(x - a_2)}{U}\right), \quad x > a_2. \tag{7.7}$$

Lighthill states that the two flows belonging to φ and $\tilde{\varphi}$ are orthogonal in a function space with the kinetic energy as norm. This means by definition that it has to be proved that for the integral I we have the orthogonality relation

$$I \overset{\text{def}}{=} \iint \left(\frac{\partial \varphi}{\partial y}, \frac{\partial \varphi}{\partial z}\right)\left(\frac{\partial \tilde{\varphi}}{\partial y}, \frac{\partial \tilde{\varphi}}{\partial z}\right) \mathrm{d}y\, \mathrm{d}z = 0. \tag{7.8}$$

Because the flows belonging to φ and $\tilde{\varphi}$ are divergenceless, we can write

$$I = \iint \operatorname{div}(\varphi \operatorname{grad} \tilde{\varphi})\, \mathrm{d}y\, \mathrm{d}z = \oint \varphi \frac{\partial \tilde{\varphi}}{\partial n}\, \mathrm{d}s, \tag{7.9}$$

where $\mathrm{d}s$ is an element of length and the contour integral is tightly around C_x and the vortex sheet. Also, a contour integral along a circle with large radius R has to be considered; however, this integral tends to zero for $R \to \infty$. It follows from (7.5) and (7.6) that $I = 0$. Thus, we have the equality

$$\begin{aligned} \iint \left(\frac{\partial \varphi}{\partial y} + \frac{\partial \tilde{\varphi}}{\partial y}\right)^2 + \left(\frac{\partial \varphi}{\partial z} + \frac{\partial \tilde{\varphi}}{\partial z}\right)^2 \mathrm{d}y\, \mathrm{d}z = \iint \left[\left\{\left(\frac{\partial \varphi}{\partial y}\right)^2 + \left(\frac{\partial \varphi}{\partial z}\right)^2\right\} + \right. \\ \left. + \left\{\left(\frac{\partial \tilde{\varphi}}{\partial y}\right)^2 + \left(\frac{\partial \tilde{\varphi}}{\partial z}\right)^2\right\}\right] \mathrm{d}y\, \mathrm{d}z \end{aligned} \tag{7.10}$$

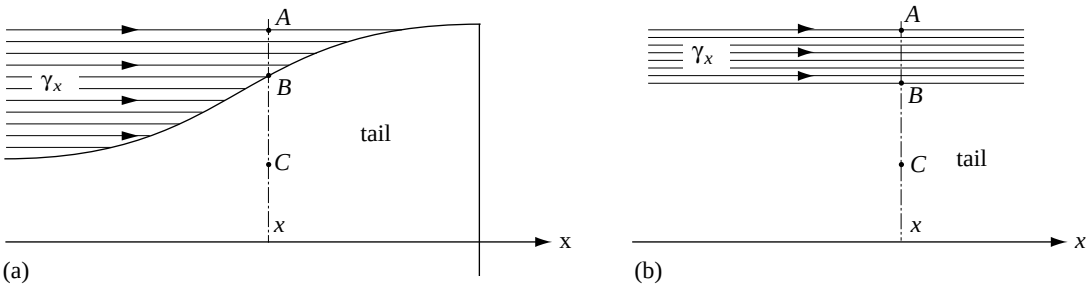

Figure 11. Tail hit by free shed vorticity sheet of width $(A - C)$, (a) real configuration, (b) two-dimensional slender-body approximation.

and for the kinetic energy $E(x,t)$ per unit of length of the flow which belongs to $\varphi + \tilde{\varphi}$ we find

$$E(x,t) = \tfrac{1}{2}m(x)V^2(x,t) + \tfrac{1}{2}\tilde{m}(x)V^2\left(a^2, t - \frac{(x-a_2)}{U}\right). \tag{7.11}$$

We now return to (7.7) by which the side force $L(x,t)$ per unit of length can, instead of (6.3), be written as

$$\begin{aligned} L(x,t) &= \left(\frac{\partial}{\partial t} + U\frac{\partial}{\partial x}\right)\left\{m(x)V(x,t) + \tilde{m}(x)V\left(a_2, t - \frac{(x-a_2)}{U}\right)\right\} = \\ &= \left(\frac{\partial}{\partial t} + U\frac{\partial}{\partial x}\right)\{m(x)V(x,t)\} + U\tilde{m}'(x)V\left(a_2, t - \frac{(x-a_2)}{U}\right). \end{aligned} \tag{7.12}$$

Because (7.7), which denotes the momentum of the fluid in the z-direction, is continuous at $x = a_2$, it follows that neither a Dirac δ-function of $\tilde{m}'(x)$ nor one of $m'(x)$ has to be taken at $x = a_2$ because they annihilate one another.

Here it is perhaps of interest to consider more explicitly the flat tail region upstream of the trailing edge of the tail. For a given x on the flat tail (Figure 11) part $(B - C)$ of the incoming free vortex sheet of width $(A - C)$ passes closely along the tail plate, while the part $(A - B)$ is above the tail plate. Following Lighthill the part $(B - C)$, which is mixed with the boundary layer of the tail, has no influence, or otherwise by its mirrored image in the tail plate it cannot induce velocities. The part $(A - B)$ of the free shed vorticity can be treated as before; however, instead of an oval body with thickness, the flat tail plate has to be taken.

When the caudal fin protrudes out of the incoming free vorticity, it follows from the foregoing that there is no influence of the incoming free vorticity sheet on the shedding of vorticity by the vertical trailing edge of the caudal fin. This shedding of vorticity remains the same as in Figure 9.

Now analogous to what was done in the first part of Section 6 up to and including (6.6), it is possible to give two representations of the energy put into the fluid by the fish. In one of these the propulsive force caused by the motions of the fish appears. Invoking the principle of conservation of energy, we can compare these two representations from which follows the propulsive force in the case of free vorticity shed by the fins.

Thus far there is one point in the analysis that deserves some thought. This concerns the orders of magnitude of the lateral dimensions of the body and its lateral movement $h(x,t)$. When these quantities have the same order of magnitude, it is doubful that the analysis of the orthogonality of the two flows belonging to the velocity potentials φ and $\tilde{\varphi}$ (7.8) is valid. Then

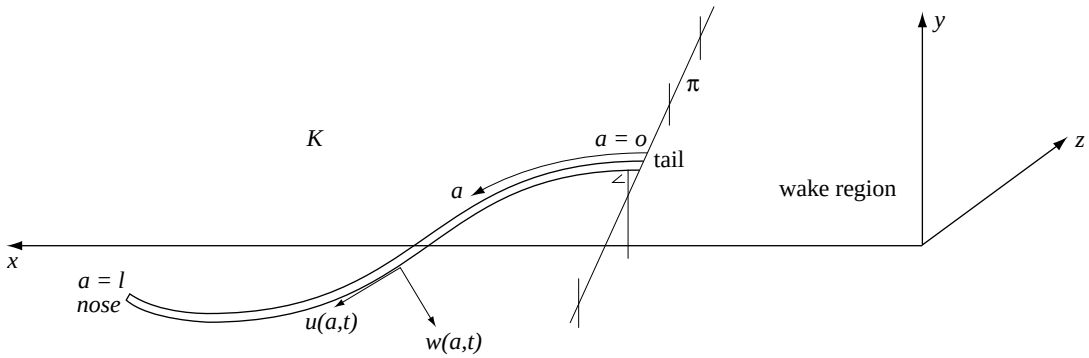

Figure 12. Spinal column of fish with length coordinate a, plane $\Pi \perp$ plane $y = 0$ and $\perp$ end of spinal column, velocity components $u(a, t)$ and $w(a, t)$ of points of spinal column, $u(a, t)$ tangential, $w(a, t)$ perpendicular to spine, both in plane $y = 0$.

it is possible that the vortex layer shed by the dorsal fin II in Figure 10 is not 'near' the plane $z = 0$. However, it can be above, beside the midplane of the body cross-section at a distance equal to the height or the width of the body cross-section, so that (7.5) cannot be used for the proof of the orthogonality property. Also, the vortex sheet under consideration can pass the tail at a distance which, for instance, is equal to the length of the trailing edge. In that case a complicated flow occurs that cannot be discussed by the given theory.

However, when we assume that the lateral motion $y = h(x, t) = O(\tilde{\epsilon})$ with $\tilde{\epsilon} \ll \epsilon$, then (7.8) will be approximately correct and also the given theory. We will return to this topic in the third paragraph below (10.19).

8. Large-amplitude elongated-body theory

We now consider a second extension of the slender-body theory of Section 6 which is with respect to the amplitude of the motion of the swimming body. This extension was given by Lighthill in his article 'Large amplitude elongated-body theory of fish locomotion' [11] mentioned above. Such an extension is of interest because the theory of Section 6 assumes that all lateral displacements and velocities are small, while in reality the lateral velocity component of the caudal fin can in certain circumstances reach values of twice the swimming velocity of the fish.

This theory is in terms of a coordinate system (x, y, z) which is at rest with respect to the undisturbed fluid at large distances of the fish. The fish moves in the neighbourhood of the plane $y = 0$; Figure 12. The fluid space is divided into two half spaces by a plane Π that is parallel to the y-axis, passes through the vertical trailing edge of the tail and is perpendicular to the end part of the tail. The half space in which the fish is present is denoted by K and the wake is assumed to remain outside K.

The spinal column is supposed to be inextensible, having a length coordinate a along it, where $a = 0$ at the tail and $a = l$ at the nose of the fish. When the spine has the representation $(x(a, t), y = 0, z(a, t))$, the inextensibility relation has the form

$$\left(\frac{\partial x}{\partial a}\right)^2 + \left(\frac{\partial z}{\partial a}\right)^2 = 1. \tag{8.1}$$

The velocity components of the points of the spine in the tangential and the normal directions are

$$u(a,t) = \frac{\partial x}{\partial t}\frac{\partial x}{\partial a} + \frac{\partial z}{\partial t}\frac{\partial z}{\partial a}, \quad w(a,t) = \frac{\partial z}{\partial t}\frac{\partial x}{\partial a} - \frac{\partial x}{\partial t}\frac{\partial z}{\partial a}, \tag{8.2}$$

respectively, reckoned positive as shown in Figure 12. Then, with respect to the (x, z) coordinate system, the components of the local momentum in the neighbourhood of the fish are given by

$$m(a,t)w(a,t)\left(-\frac{\partial z}{\partial a}, \frac{\partial x}{\partial a}\right), \tag{8.3}$$

where $m(a,t)$ is the virtual mass per unit of length of the cross-section of the fish at a. Lighthill assumes that $m(a,t)$ depends also on time, which is important for fish with a caudal fin with the length of its trailing edge changing during a swimming cycle. The way in which $m(a,t)$ has to be defined is possibly still open for discussion. The reason is that the deforming body has no 'self-evident' velocity, which in the general case makes the time-dependent virtual mass a concept that has to be used with care.

Now the theory considers the rate of change of momentum within the half space K bounded by the plane Π. The momentum follows approximately from (8.3) by an integration over $0 \le a \le l$. The rate of change is then obtained by a differentiation of the result with respect to time and, quoting Lighthill, has to be equal to the sum of the following three quantities :

(i) The rate of change of momentum due to convection out of K across the plane Π;

(ii) The rate of change of momentum due to the pressure force acting across the plane Π;

(iii) Minus the reaction force (T, L) with which the fluid acts on the fish.

This results in the equation

$$\frac{\mathrm{d}}{\mathrm{d}t}\int_0^l mw\cdot\left(-\frac{\partial z}{\partial a}, \frac{\partial x}{\partial a}\right)\mathrm{d}a = \left[-u\cdot(mw)\left(-\frac{\partial z}{\partial a}, \frac{\partial x}{\partial a}\right) + \tfrac{1}{2}mw^2\cdot\left(\frac{\partial x}{\partial a}, \frac{\partial z}{\partial a}\right)\right]\Bigg|_{a=0} - (T, L). \tag{8.4}$$

Lighthill argues that the only flux of momentum through the plane Π follows from the translation of Π with the velocity component $u(0,t)$, which is normal to Π. This is per second the amount $u\cdot(mw)$ in the direction of the unit normal on the tail $(-\partial z/\partial a, \partial x/\partial a)$ which yields the first term at the right-hand side of (8.4). The second term is caused by the pressures acting at K across Π of which a clear derivation is given by Childress in his book 'Mechanics of swimming and flying' [15].

Rewriting the expression between square brackets in (8.4) as

$$mw\left\{-u\cdot\left(-\frac{\partial z}{\partial a}, \frac{\partial x}{\partial a}\right) + w\cdot\left(\frac{\partial x}{\partial a}, \frac{\partial z}{\partial a}\right)\right\} - \tfrac{1}{2}mw^2\cdot\left(\frac{\partial x}{\partial a}, \frac{\partial z}{\partial a}\right) \tag{8.5}$$

and using (8.1) and (8.2), we find that (8.4) can be written as

$$(T, L) = \left\{mw\cdot\left(\frac{\partial z}{\partial t}, -\frac{\partial x}{\partial t}\right) - \tfrac{1}{2}mw^2\cdot\left(\frac{\partial x}{\partial a}, \frac{\partial z}{\partial a}\right)\right\}\Bigg|_{a=0} - \frac{\mathrm{d}}{\mathrm{d}t}\int_0^l mw\cdot\left(-\frac{\partial z}{\partial a}, \frac{\partial x}{\partial a}\right)\mathrm{d}a. \tag{8.6}$$

Because the last term in (8.6) is periodic with respect to time, the mean thrust $\overline{T}$, when the fish swims in the x-direction, becomes

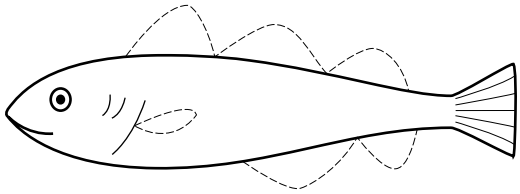

Figure 13. Cod used as test fish in swimming-power measurements. During fast swimming the dotted fins have collapsed against the body. From Wardle and Reid [16].

$$\overline{T} = \left.\overline{\left\{ mw \cdot \left(\frac{\partial z}{\partial t} - \tfrac{1}{2} w \frac{\partial x}{\partial a} \right) \right\}}\right|_{a=0}, \tag{8.7}$$

which is a rather simple result for a complicated problem.

Up to now the recoil conditions did not enter into the discussion. These conditions are related to the time-dependent side force L acting on the fish, which follows from (8.6). Lighthill discusses that recoil motions will be relatively small when the fish has a good height of the front part of its body and has a substantial reduction of the height in front of the tail.

An estimate is given of the kinetic energy left behind in the wake. The kinetic energy in this theory per unit of length in the neighbourhood of the trailing edge of the tail is $(\frac{1}{2}mw^2)|_{a=0}$. Because the tangential velocity of the trailing edge is $u(0, t)$, an estimate of the mean kinetic energy $\overline{E}$ leaving the tail per second and shed into the fluid behind the fish, becomes

$$\overline{E} = \left.\overline{(\tfrac{1}{2}mw^2 u)}\right|_{a=0}. \tag{8.8}$$

In 'The application of large amplitude elongated-body theory to measure swimming power in fish' [16] Wardle and Reid used this theory to arrive at an estimate of the swimming power of fish. For their experiments they used a cod (Figure 13) of length 73·4 cm and weight 3·2 kg, swimming at a speed of about 3 m/s with its median fins folded . We quote their appraisal of the results: 'The direct application of the reactive theory to measure swimming power in fish appears to give results that are in agreement with both biochemical assessment of power available and estimates based on drag to be overcome by swimming'.

9. Balistiform locomotion

In the article 'Biofluid dynamics of balistiform and gymnotiform locomotion, Part I. Biological background and analysis by elongated-body theory' by Lighthill and Blake [17] several aspects of the balistiform swimming of fish are considered; in this section we will discuss some of these.

As we mentioned briefly in the Introduction, the balistiform kind of locomotion is caused by undulations propagated along flexible dorsal and anal fins, while the body and the tail fin are rigid and remain straight; Figure 14. For the calculation of the propulsive force **F** Lighthill and Blake use, as in the elongated-body theory of Section 8, a vertical plane Π separating the half space K in which the propulsive fins are active from the half space in which the wake is present. In the case of balistiform locomotion the plane Π is placed at the posterior end of the propulsive apparatus formed by the dorsal and anal fins, so that the rigid caudal fin is in the half space of the wake. Further, it is demanded that the plane Π is such that the local fluid momentum vector **M**, occurring at the posterior end of the propulsive fins, lies in Π. Then, in general, Π will be in an oblique position with respect to the backbone.

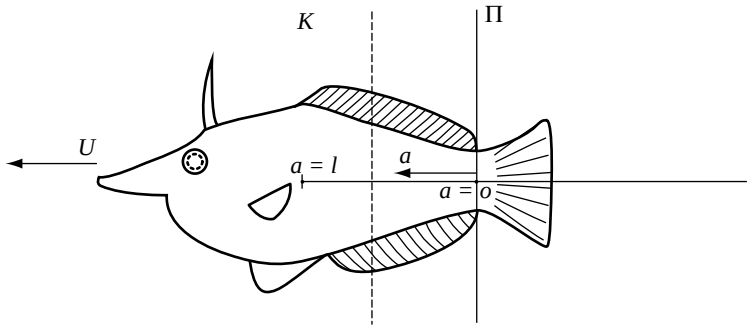

Figure 14. Fish with balistiform locomotion, Oxymonacanthus longirostris, - - - - - - - cross-section used in Figure 15. Based on Lighthill and Blake [17].

Along the fish a length parameter a has been defined with $a = 0$ at Π and $a = l$ at the anterior end of the propulsive fins. Then again the following balance of momentum is valid for the half space K

$$\frac{\mathrm{d}}{\mathrm{d}t}\int_0^l \mathbf{M}\,\mathrm{d}a = -\mathbf{F} + \mathbf{P} - U(\mathbf{M})\Big|_{a=0}, \tag{9.1}$$

where at the left-hand side the rate of change of momentum in K is given, and at the right-hand side $\mathbf{F}$ is the propulsive force, $\mathbf{P}$ is the pressure force across the plane Π, $(\mathbf{M})|_{a=0}$ is the local momentum per unit of length caused by the motion of the fins and U is the swimming velocity of the fish. In a periodic motion the mean value with respect to time of the left-hand side of (9.1) is zero, hence for the mean values with respect to time of the other quantities the following holds

$$\overline{\mathbf{F}} = -U\overline{(\mathbf{M})}\Big|_{a=0} + \overline{\mathbf{P}}. \tag{9.2}$$

Lighthill and Blake proceed by describing a simple mathematical model from which it can be understood why this form of propulsion has the capacity of providing relatively high speeds, although the body and the tail fin remain rigid and in one plane. In this model the body is, for the sake of simplicity, assumed to have no thickness and to be flat. A cross-section of the body is considered, see dashed line in Figure 14, which cuts the dorsal fin and the anal fin. The height of the body is $2s$ and each fin has a width $(l - s)$. The flow caused by the motion of the two fins is assumed to be two-dimensional. The situation of Figure 15a is considered, which can be generalized to the problem of Figure 16 for the calculation of the momentum M in the y-direction per unit of length, when the velocity of the flexible plate is $v_y = f(x)$. Hence, the velocity potential $\varphi(x, y)$, which satisfies the two-dimensional Laplace equation, satisfies the boundary condition

$$\frac{\partial\varphi}{\partial y} = f(x), \quad -l < x < l, \tag{9.3}$$

while the circulation around the plate has to be taken equal to zero.

In the first instance we treat this problem differently from [17] in order to avoid an integral in the (x, y)-plane for the momentum in the y-direction that is not absolutely convergent. Instead of the time-independent problem we consider a time-dependent problem with $v_y = 0$ for $t < 0$ and with $v_y = f(x)$ for $t \geq 0$. We introduce the time-dependent potential

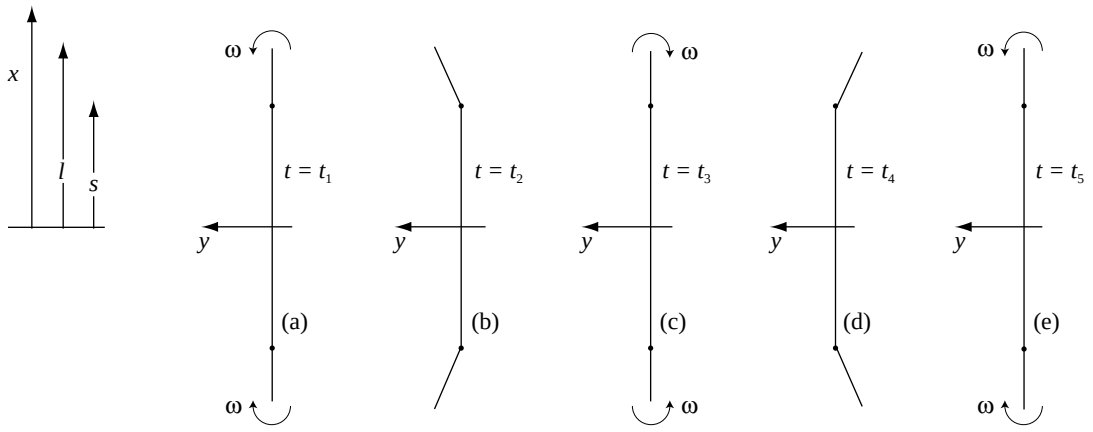

Figure 15. Cross-section of fish; see dashed line Figure 14; one cycle of the motion of the fins; ω is radian rotational velocity of fins. Based on Lighthill and Blake [17].

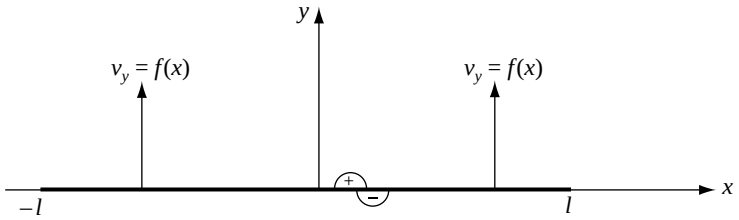

Figure 16. The two-dimensional flow with $v_y = f(x)$, $-l \leq x \leq l$, $y = 0$.

$\tilde{\varphi}(x, y, t) = \varphi(x, y)H(t)$, where $H(t)$ is the step function $H(t) = 0$ for $t < 0$ and $H(t) = 1$ for $t \geq 0$. The pressure in the fluid follows from the unsteady Bernoulli equation:

$$p(x, y, t) = -\rho \frac{\partial \tilde{\varphi}}{\partial t} - \tfrac{1}{2}\rho \left\{ \left(\frac{\partial \tilde{\varphi}}{\partial x} \right)^2 + \left(\frac{\partial \tilde{\varphi}}{\partial y} \right)^2 \right\}. \tag{9.4}$$

Because $(\partial\tilde{\varphi}/\partial x)^2$ and $(\partial\tilde{\varphi}/\partial y)^2$ are symmetric with respect to y, we find for the pressure jump over the plate

$$[p]_-^+ = (p^+ - p^-) = -\rho\{\varphi^+(x, 0)\delta(t) - \varphi^-(x, 0)\delta(t)\} = -2\rho\varphi^+(x, 0)\delta(t), \tag{9.5}$$

where $\delta(t)$ is the Dirac delta function. Hence, the resultant force $L(t)$ in the y-direction to be exerted on the fluid at the plate has the value

$$L(t) = -2\rho\delta(t) \int_{-l}^{l} \varphi^+(x, 0)\, \mathrm{d}x. \tag{9.6}$$

Then the momentum M of the fluid in the y-direction for $t = +0$ becomes

$$M = \int_{-\epsilon}^{\epsilon} L(t)\, \mathrm{d}t = -2\rho \int_{-l}^{l} \varphi^+(x, 0)\, \mathrm{d}x = \rho \oint_{-l}^{l} \varphi(x, 0)\, \mathrm{d}x, \tag{9.7}$$

where the contour integration is around the plate in an anti-clockwise direction. This is the same result as in [17, Formula 6], which we follow again henceforth.

Lighthill and Blake reduce expression (9.7) to an attractively simple form. Consider the potential $\varphi_1(x, y)$ for $f(x) = 1$, hence with $\partial\varphi_1(x, 0)/\partial y = 1$ for $-l \leq x \leq l$. Then, instead of (9.7), we can write

$$M = \rho \oint \varphi(x,0)\frac{\partial \varphi_1}{\partial y}(x,0)\,\mathrm{d}x = \rho \oint \varphi_1(x,0)\left(\frac{\partial}{\partial y}\varphi(x,y)\right)\Big|_{y=0}\mathrm{d}x, \tag{9.8}$$

where Green's theorem is used in the second equality. The limit values of $\varphi_1(x, y)$ for $y \to 0$ can be calculated easily, for instance by means of a solvable singular integral equation; they are

$$\varphi_1(x, \pm 0) = \mp(l^2 - x^2)^{1/2}. \tag{9.9}$$

The announced simple form of (9.8) now becomes

$$M = 2\rho \int_{-l}^{l} (l^2 - x^2)^{1/2} f(x)\,\mathrm{d}x. \tag{9.10}$$

The function $f(x)$ for the case of Figure 15a is

$$f(x) = 0, \quad |x| < s; \quad f(x) = \omega \cdot (|x| - s), \quad s \le |x| \le l. \tag{9.11}$$

where ω is the angular velocity of the fins. Then by (9.10) the momentum M becomes

$$M = 2\rho\omega\{\tfrac{1}{3}(l^2 - s^2)^{1/2}(2l^2 + s^2) - sl^2\ \cos^{-1}(s/l)\}. \tag{9.12}$$

Formula (9.10) can also be used for the calculation of the momentum $\frac{1}{2}M_0$ in the y-direction by one fin of length $(l - s)$, whence we find for the two fins without the body in between and no other interaction

$$M_0 = \frac{\pi}{4}\rho\omega(l - s)^3. \tag{9.13}$$

Hence, by the presence of the body for $|x| \le s$ and the nearness of the fins, there is an amplification of the induced momentum in the y-direction by a factor $\beta = M/M_0$. This factor β is drawn in Figure 17 and is called by Lighthill and Blake the main result of their paper. It shows that the two fins attached to the flat rigid body can generate considerably more momentum than two fins 'free in space' without interaction.

This is, of course, not a useful model for balistiform locomotion, because the two fins drawn in Figure 15 induce two-dimensional momentum in the lateral y-direction without a propulsive component in the posterior direction of the fish. This can be changed by recognizing that the real motion of the two fins is more or less undulatory, by which the normal at the high-pressure side of a fin can have a component in the posterior direction of the fish. Then a thrust component can arise.

Lighthill and Blake enter deeply into the propulsive consequences of the foregoing and give expressions for the quantities $\overline{\mathbf{M}}$ and $\overline{\mathbf{P}}$ occuring in (9.2) by which the mean propulsive force can be determined. For this we refer to their paper.

In three subsequent papers [18] Lighthill elaborates the problem further and discusses the presence of a body with elliptical cross-section and the effect of short-wavelength undulations of the fins. In the latter case the two-dimensional theory no longer holds for the calculation of the enhancement factor β of Figure 17. This factor will be reduced because neighbouring opposite amplitudes at the dorsal or the anal fin will hinder each other in inducing a large momentum in the lateral direction. Lighthill discusses that in this case it is better not to use the two-dimensional Laplace equation but rather

$$\frac{\partial^2 \varphi}{\partial x^2} + \frac{\partial^2 \varphi}{\partial y^2} - k^2\varphi = 0, \tag{9.14}$$

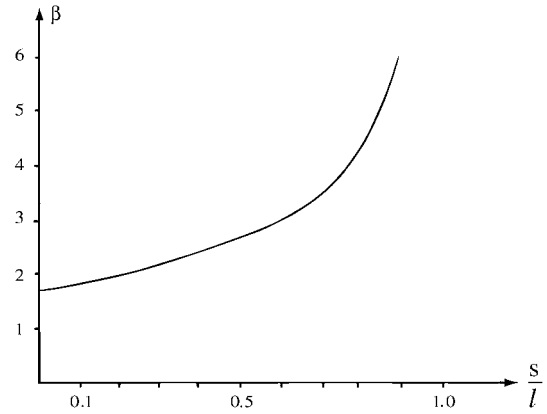

Figure 17. The momentum enhancement factor β. From Lighthill and Blake [17].

where $k = 2\pi/\lambda$ and λ is the wavelength of the undular motion of the fins.

10. More about vorticity shedding in slender-body theory

After discussing in the preceding four sections mainly the pioneering work of Lighthill on the swimming of fish, we will discuss in the next two sections some of the profound work of T.Y. Wu. After his early paper [7] of 1961, Wu published in 1971 'Hydromechanics of swimming propulsion' [19] of which we consider here 'Part 3. Swimming movements of slender fish with side fins'.

In that paper the fish is assumed to have zero thickness and the mathematics shows an interesting application of the theory of complex functions. However, among other things, we will discuss that, for the region where the tail is struck by shed vorticity, the analysis is not valid. This was remarked by Wu and Newman in their subsequent paper 'Unsteady flow around a slender fish-like body' [20] where they give a solution of the more general problem of a slender fish with thickness.

Notwithstanding the mentioned shortcoming, the theory developed in [19, Part 3] is elucidating, because its subject can be formulated in a nice and simple manner and is solved partly explicitly in an elegant way. So we consider the fundamental Section 2 of that paper.

As mentioned before, the fish is assumed to have zero thickness, its planform S_b (x, y) is part of the (x, y)-plane, the upper and lower boundaries of S_b are $y = b(x) \geq 0$ and $y = -b(x) \leq 0$, respectively. The nose of the fish is at $x = -l_n$, at $x = 0$ we have $b'(x) = 0$, the tail base neck is at $x = 1$ and the vertical trailing edge of the tail is at $x = l$. The lateral motion of the body is $z = h(x, t) = O(\epsilon)$. The velocity of the incoming fluid in the positive x-direction is U and the perturbation velocity field is (u, v, w).

The sharp leading edges of the 'body' S_b of the fish (including the tail) for $-l_n < x < 0$ and for $1 < x < l$ will have a square-root singularity of the pressure, while at the trailing edges of S_b for $0 < x < 1$ and at $x = l$, the Kutta condition for smooth flow will be imposed. At these trailing edges, free vorticity is shed into the fluid, which is transported with velocity U in the positive x-direction.

The velocity potential $\varphi(x, y, z, t)$ of the perturbation velocities (grad $\varphi = (u, v, w)$) satisfies the three-dimensional Laplace equation; however, in concurrence with slender-body theory it is again assumed that φ has to satisfy only the two-dimensional Laplace equation

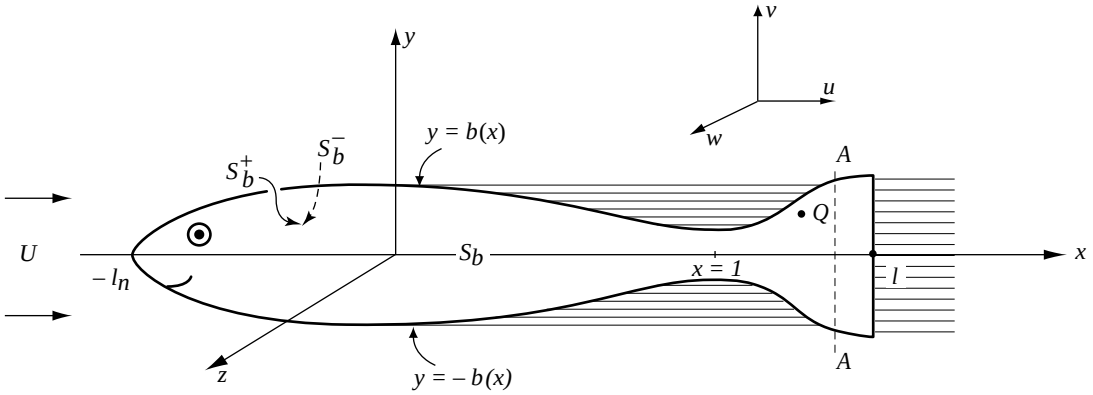

Figure 18. Fish body S_b in the neighbourhood of the (x, y) plane.

$$\frac{\partial^2\varphi}{\partial y^2} + \frac{\partial^2\varphi}{\partial z^2} = 0. \tag{10.1}$$

Therefore the complex potential $f(\zeta; x, t) = \varphi + \mathrm{i}\psi$ can be introduced and $\mathrm{d}f/\mathrm{d}\zeta = v - \mathrm{i}w$ where $\zeta = y + \mathrm{i}z$ and $\psi(x, y, z, t)$ is the stream function which is conjugated to φ, $(\partial\varphi/\partial y = \partial\psi/\partial z, \partial\varphi/\partial z = -\partial\psi/\partial y)$.

Wu also introduces the acceleration potential $\Phi = -p/\rho$ where p is the pressure, which we assume here to be zero at infinity. By using the equation of motion

$$\frac{\partial u}{\partial t} + U\frac{\partial u}{\partial x} = \frac{\partial\Phi}{\partial x}, \tag{10.2}$$

and putting $u = \partial\varphi/\partial x$, we obtain by integration of this equation with respect to x from $x = -\infty$ (where $\varphi = 0$) to x:

$$\Phi = \left(\frac{\partial}{\partial t} + U\frac{\partial}{\partial x}\right)\varphi = \mathrm{D}\varphi, \quad \mathrm{D} = \left(\frac{\partial}{\partial t} + U\frac{\partial}{\partial x}\right). \tag{10.3}$$

Hence Φ is also harmonic with respect to y and z and has a conjugated function Ψ. The functions $f(\zeta; x, t)$ and $F(\zeta; x, t) = \Phi(x, y, z, t) + \mathrm{i}\Psi(x, y, z, t)$ are then sectionally holomorfic functions of ζ; the line segments on which they have discontinuities will become clear in the course of the analysis.

It follows from (10.3) that

$$F(\zeta; x, t) = \mathrm{D}f(\zeta; x, t) \to \frac{\mathrm{d}F}{\mathrm{d}\zeta} = \mathrm{D}\frac{\mathrm{d}f}{\mathrm{d}\zeta} = \mathrm{D}(v - \mathrm{i}w) = \mathrm{D}\Omega(\zeta; x, t), \tag{10.4}$$

where $\Omega = v - \mathrm{i}w$ is introduced.

First the front part $-l_n < x < 0$ of the body S_B is considered. The complex velocity Ω satisfies at S_B the boundary condition (see (6.1)) for a fixed value of x

$$\Im\mathrm{m}\ \Omega(\zeta; x, t) = -w = -\left(\frac{\partial}{\partial t} + U\frac{\partial}{\partial x}\right)h(x, t) = -V(x, t), \quad -l_n < x < 0, |y| < b(x), z = 0. \tag{10.5}$$

Hence, because $v(x, y, z, t) = -v(x, y, -z, t)$, we can formulate for Ω the Hilbert problem in the complex $\zeta = y + \mathrm{i}z$ plane for fixed x

$$\Omega^+ + \Omega^- = -2\mathrm{i}V(x,t); \quad -l_n < x < 0, \quad |y| < b(x), z = 0, \tag{10.6}$$

where $\Omega^+(\Omega^-)$ means the limit of Ω for $z \to 0$ at the $S_b^+(S_b^-)$ side of S_b (Figure 18).

This Hilbert problem can be solved explicitly by the method given by Muskhelishvily in 'Singular integral equations' [21, p.227 and further]. It is found that the solution with the desired singularity at the leading edge $y = \pm b(x), -l_n < x < 0$, that vanishes at $\zeta = \infty$ becomes

$$\Omega(\zeta; x, t) = \frac{\mathrm{d}f}{\mathrm{d}\zeta}(\zeta; x, t) = \mathrm{i}V(x,t)[\zeta\{\zeta^2 - b^2(x)\}^{-1/2} - 1], \quad -l_n < x < 0, \tag{10.7}$$

where the branch of the square root is determined by choosing for the root a positive real value for $y > b(x)$ and $z = 0$. The complex velocity potential $f(\zeta)$ follows from an integration of (10.7)

$$f(\zeta; x, t) = \varphi + \mathrm{i}\psi = \mathrm{i}V(x,t)[\{\zeta^2 - b^2(x)\}^{1/2} - \zeta] \to F(\zeta; x, t) = \mathrm{D}f(\zeta; x, t),$$

$$0 < x < 1, \tag{10.8}$$

where in the last equality (10.4) has been used.

Next the region $0 < x < 1$ of S_b is considered which has the trailing edges $y = \pm b(x)$ where the Kutta condition has to be satisfied. Here Wu makes the crucial choice to start not with Ω but with $\mathrm{d}F(\zeta; x, t)/\mathrm{d}\zeta$, which by (10.4) and (10.5) must satisfy the boundary condition for fixed x

$$\Im\mathfrak{m}\frac{\mathrm{d}F}{\mathrm{d}\zeta}(\zeta; x, t) = -\mathrm{D}w(x, y, 0, t) = -\mathrm{D}V(x,t), \quad 0 < x < 1, \quad |y| < b(x), \quad z = 0. \tag{10.9}$$

Hence, for $\mathrm{d}F/\mathrm{d}\zeta$, by the anti-symmetry of v with respect to y and by the continuity of w, the following holds:

$$\left(\frac{\mathrm{d}F}{\mathrm{d}\zeta}\right)^+ + \left(\frac{\mathrm{d}F}{\mathrm{d}\zeta}\right)^- = -2\mathrm{i}DV(t); \quad 0 < x < 1, \quad |y| < b(x), \quad z = 0. \tag{10.10}$$

Further we have

$$\left(\frac{\mathrm{d}F}{\mathrm{d}\zeta}\right)^+ - \left(\frac{\mathrm{d}F}{\mathrm{d}\zeta}\right)^- = \mathrm{D}\{(v^+ - v^-) - \mathrm{i}(w^+ - w^-)\} = 2Dv^+ = 0, \quad b(x) < y < b(0),$$

$$z = 0, \tag{10.11}$$

where in the last equality we have used that the free vorticity has to be transported by the incoming parallel flow of velocity U. From this it is found that $\mathrm{d}F/\mathrm{d}\zeta$ is analytic with the exception of $(|y| < b(x), z = 0)$ and we obtain for $\mathrm{d}F/\mathrm{d}\zeta$ the Hilbert problem (10.10). In agreement with (10.6), (10.7) and (10.8) the following $F(\zeta)$ arises

$$F(\zeta; x, t) = \mathrm{i}(DV(x,t))[\{\zeta^2 - b^2(x)\}^{1/2} - \zeta], \quad 0 < x < 1, \tag{10.12}$$

which is a continuous continuation at $x = 0$ of the $F(\zeta; x, t)$ given in (10.8) when $\mathrm{d}b(x)/\mathrm{d}x = 0$ for $x = 0$, as is assumed in Figure 18.

Then, $f(\zeta; x, t)$ can be obtained as the solution of the first equality of (10.4); after some manipulations it is found that

$$f(\zeta; x, t) = \mathrm{i}V\left(0, t - \frac{x}{U}\right)\{\zeta^2 - b^2(0)\}^{1/2} - \mathrm{i}V(x, t)\zeta + \mathrm{i}\int_0^x \{\zeta^2 - b^2(\xi)\}^{1/2} \cdot \frac{\partial}{\partial \xi} V\left(\xi, t + \frac{(\xi - x)}{U}\right) \mathrm{d}\xi. \tag{10.13}$$

From this $f(\zeta; x, t)$ it can be checked that the normal component of the velocity at the body of the fish for $0 < x < 1$ is equal to $V(x, t)$, that the x-component of vorticity $\gamma_x = -2v^+$ at the body at $y = b(x)$ is continued in the wake and that this vorticity in the wake is transported in the x-direction with velocity U.

For the tail region $1 < x < l$ of the body of the fish the following representation of the complex velocity potential $f(\zeta; x, t)$ is chosen in [19]

$$f(\zeta; x, t) = \mathrm{i}V(x, t)[\{\zeta^2 - b^2(x)\}^{1/2} - \zeta] + g(\zeta; x - Ut), \tag{10.14}$$

where $g(\zeta; x - Ut)$ is still an arbitrary function of its two arguments. However, this representation is not sufficiently general. It yields a contradiction when we suppose, for instance, that $h(x, t) = 0$ for $1 < x < l$ by which $f(\zeta; x, t) = g(\zeta; x - Ut)$. When the tail is sufficiently wide ($> b(0)$) and long, the slender-body theory yields $f(\zeta; x, t) = 0$ for the dashed cross-section $A - A$ of Figure 18 and for cross-sections downstream of it. This is contrary to the fact that $g(\zeta; x - Ut) \neq 0$ at points for which $1 < x < l$, where free shed vorticity is transported and then $g(\zeta; x - Ut) \neq 0$ for all downstream values of x.

That indeed wrong results are obtained when using (10.14) can be seen from Wu's formula (28) when, for instance, the following choice is made

$$h(x, t) = \frac{1}{U}(x + l_n) \sin\ (x - Ut). \tag{10.15}$$

Then it is found that for a point $Q(x, y)$ (Figure 18) on the tail with $(1 < x < l, b(1) < y < b(x))$ the velocity component w normal to the tail becomes

$$w(x, y, t) = V(x, y, t)\left\{1 + \frac{y}{(y^2 - b^2(1))^{1/2}}\right\} > 2V(x, t) \tag{10.16}$$

instead of the required $w = V(x, t)$.

Up to and including (10.13) the theory is correct within the formal framework of slender-body theory for fish of which the body planform is convex and the theory gives a nice and explicit solution for the perturbation velocities, pressures and so on, although the recoil conditions still have to be considered.

However, the tail region $1 < x < l$ can be treated the way Wu and Newman did this in their already mentioned paper [20] by means of the Riemann–Hilbert problem which we will discuss now. For the sake of simplicity we will take the width of the tail smaller than $b(0)$.

For the complex velocity function $\Omega(\zeta; x, t) = v - \mathrm{i}w$ we can deduce boundary conditions along the complete real y-axis. First we have, as before,

$$\mathfrak{Im}\ \Omega^+(\zeta; x, t) = -V(x, t), \quad 1 < x < l, \quad -b(x) < y < b(x), \quad z = +0. \tag{10.17}$$

For the intervals $(-b(0) < y < -b(x))$ and $(b(x) < y < b(0))$, Equation (10.13) yields the two shed free-vorticity sheets, which we denote by $\gamma_{x_1}(x - Ut, y)$ and $\gamma_{x_2}(x - Ut, y)$, respectively. The parts of these vorticity sheets that are at the considered cross-section x, already alongside of the tail, are neglected; see Figure 11 and its discussion. Then the velocity components in the y-direction, $v_1^+ = -\frac{1}{2}\gamma_{x_1}$ and $v_2^+ = -\frac{1}{2}\gamma_{x_2}$, are known at these intervals, by which

$$\Re\mathfrak{e}\ \Omega^+(\zeta; x, t) = v_1^+(v_2^+), \quad 1 < x < l, \quad -b(0) < y < -b(x),\ (b(x) < y < b(0)),$$
$$z = +0. \tag{10.18}$$

Finally, for the intervals $(-\infty < y < b(0))$ and $(b(0) < y < \infty)$, the velocity component v in the y-direction is zero because in the configuration only vorticity for $-b(0) < y < b(0)$ and $z = 0$ is present. So for these intervals we have

$$\Re\mathfrak{e}\ \Omega^+(\zeta; x, t) = 0, \quad 1 < x < l, \quad -\infty < y < -b(0) \quad \text{or} \quad b(0) < y < \infty, \quad z = +0. \tag{10.19}$$

For each fixed x and t Equations (10.17), (10.18) and (10.19) form a Riemann–Hilbert problem for the function $\Omega(\zeta; x, t)$, the solution of which is explicitly given by Muskhelishvily in [21, p.109–111]. It is important that the solution of the homogeneous equation needed in the analysis is symmetric with respect to y, so that no non-zero circulation around the tail region will occur.

In their paper 'A generalized slender-body theory for fish-like forms' [22] Newman and Wu proceed by studying the interaction of a slender body with the free vorticity shed by appended lifting surfaces or fins. Here the body has also thickness. The starting point of the theory, which uses again complex function theory, is the method introduced by Lighthill that was discussed in Section 6 (Equations (6.8)–(6.14)) where the time-dependent coordinate transformation was used that transforms the moving body into a time-independent shape.

In [22] – see also the remark at the end of Section 7 – apparently two orders of magnitude are used, namely δ for the lateral dimensions of the slender body, which are $O(\delta)$ and h for the lateral motion $h(x, t) = O(h)$. An approximation for the pressure in the fluid is obtained by using in the expansion terms up to and including $O(\delta h)$, while, among other things, terms of $O(h^2)$ are neglected. This means that the amplitude of the lateral motion $h(x, t)$ is assumed to be much smaller than the lateral dimensions of the slender body.

Then it is shown that, under these assumptions, the vorticity shed by the fins follows, within the stated accuracy, the streamlines along the stretched body placed in the incoming parallel flow with velocity U. The paper discusses, for instance, the lift force on a body with fins that translates under a constant angle of attack.

We mention also the article 'The force on a slender fish-like body' [23] by Newman. The first part of it gives a clear and classical approach to the formulation of the forces caused by any type of swimming body which is allowed to have a large-amplitude motion and is possibly equiped with fins. It is related to the problem discussed by Lighthill [11] (Section 8 of this survey) and, in some sense, gives a generalization of the results.

11. Accelerated swimming of a flexible plate. Two-dimensional theory

The papers 'Swimming of a waving plate' [7] and 'Hydrodynamics of swimming propulsion. Part I. Swimming of a two-dimensional flexible plate at variable forward speeds in an inviscid fluid' [19] are also two fundamental papers by T.Y. Wu for the understanding of the swimming of fish. We will discuss the second one because it is a generalization of the first and, besides this, it uses the transparent method of the theory of sectionally holomorfic functions.

The two-dimensional theory discusses the swimming of a flexible plate of zero thickness and infinite span in a flow with a time-dependent incoming velocity $U(t)$. In others words, it can describe the accelerated swimming of the plate in a fluid at rest. Although there are

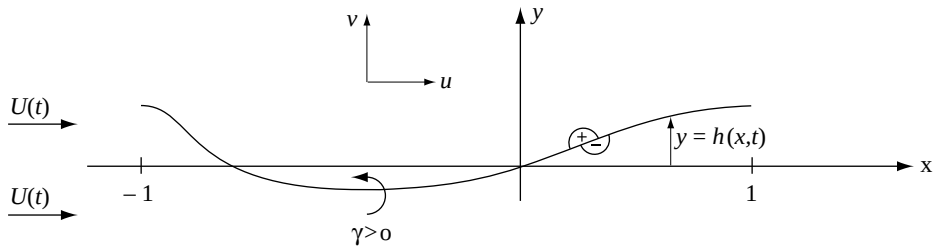

Figure 19. The swimming flexible plate.

no two-dimensional fish, the theory can be used to obtain insight in the propulsion of, for instance, porpoises, whales and sharks, which have a tail with a large aspect ratio.

The lateral motions of the plate (Figure 19) in the y-direction are assumed to start at $t = 0$ and to be small

$$y = h(x, t) = O(\epsilon), \quad -1 < x < 1, \quad 0 < t. \tag{11.1}$$

A difficulty is that the flow is considered with respect to a non-inertial coordinate system (x, y, t) which, with respect to the inertial system, say (X, Y, T), has a velocity $U(t)$ in the negative X-direction. Because $U(t)$ is a function of t, the system (x, y, t) has accelerations in the X-direction. However, we can start with the (X, Y, T)-system and consider the nonlinear equations of motion. Then, by the transformation

$$x = X + \int_0^t U(\tilde{t})\, \mathrm{d}\tilde{t}, \quad y = Y, \quad t = T, \tag{11.2}$$

we can transform the equations of motion, which are then valid with respect to the (x, y, t)-system. After this we linearize these latter equations, from which the starting equations of Wu arise, namely

$$\frac{\partial u}{\partial t} + U(t)\frac{\partial u}{\partial x} = -\frac{1}{\rho}\frac{\partial p}{\partial x}, \quad \frac{\partial v}{\partial t} + U(t)\frac{\partial v}{\partial x} = -\frac{1}{\rho}\frac{\partial p}{\partial y}. \tag{11.3}$$

Differentiating the first equation in (11.3) with respect to x and the second with respect to y and using div $(u, v) = 0$, we find

$$\frac{\partial^2 p}{\partial x^2} + \frac{\partial^2 p}{\partial y^2} = 0; \tag{11.4}$$

hence the perturbation pressure is a harmonic function. Then, the harmonic Prandtl acceleration potential $\varphi(x, y, t) = -p/\rho$ is introduced with $p = 0$ at infinity.

Because there is only vorticity at $y = 0$, we have $u(x, y, t) = -u(x, -y, t)$, hence by the first equation of (11.3) and by integrating from $x = -\infty$ towards x, we find that the acceleration potential is an odd function of y, or $\varphi(x, y, t) = -\varphi(x, -y, t)$.

Outside the line segment $(-1 < x < B(t), y = 0)$, where $B(t) > 1$ is the end of the vorticity shed by the flexible plate, the velocity field is free of rotation and hence is the gradient of a harmonic potential. Thus, also u and v are harmonic functions and by rot $(u, v) = 0$ and div $(u, v) = 0$ they are conjugate harmonic functions, hence $w(z, t) = u - \mathrm{i}v$ is an analytic function of $z = x + \mathrm{i}y$, outside the mentioned line segment.

There also exists a harmonic function $\psi(x, y, t)$ that is conjugated to the acceleration potential $\varphi(x, y, t)(\partial\varphi/\partial x = \partial\psi/\partial y, \partial\varphi/\partial y = -\partial\psi/\partial x)$. Hence, the analytic complex

acceleration potential $f(z,t) = \varphi + \mathrm{i}\psi$ can be formed. From this Wu writes the linearized equations of motion (11.3) as

$$\frac{\partial f}{\partial z} = \frac{\partial w}{\partial t} + U(t)\frac{\partial w}{\partial z}. \tag{11.5}$$

Taking for instance $\partial/\partial z = \partial/\partial x$, using the conjugate relations and comparing the real and imaginary parts of (11.5), we recover Equations (11.3).

The linearized boundary conditions at the flexible plate then become

$$v(x,+0,t) = v(x,-0,t) = \frac{\partial h}{\partial t} + U(t)\frac{\partial h}{\partial t} = V(x,t), \quad |x| < 1, \quad y = 0, \tag{11.6}$$

$$-\frac{\partial \psi}{\partial x} = \frac{\partial \varphi}{\partial y} = -\frac{1}{\rho}\frac{\partial p}{\partial y} = \frac{\partial v}{\partial t} + U(t)\frac{\partial v}{\partial x} = \left(\frac{\partial}{\partial t} + U(t)\frac{\partial}{\partial x}\right) V(x,t), \quad |x| < 1, \quad y = 0, \tag{11.7}$$

$$\varphi(x,0,t) = 0, \quad |x| > 1, \quad y = 0, \tag{11.8}$$

$$|f(1,t)| < \infty, \quad \forall t; \qquad \lim_{|z|\to\infty} f(z,t) = 0; \qquad \lim_{|z|\to\infty} w(z,t) = 0. \tag{11.9}$$

Now Wu replaces the time t by a parameter τ defined by

$$\tau = \int_0^t U(t_1)\,\mathrm{d}t_1, \tag{11.10}$$

and it is assumed that $U(t)$ is such that for each t there is a unique τ and there is an inverse function $t = t(\tau)$. This holds for $U(t) > 0$ and then the shed vorticity in the wake cannot be transported back to the plate. In the following $U(t(\tau))$ is denoted by $U(\tau)$, although $U(t)$ and $U(\tau)$ are different functions of their arguments. The same will hold also for some other functions, for instance $f(z,t(\tau))$ is denoted by $f(z,\tau)$.

Then Wu introduces

$$F(z,\tau) = f(z,\tau)/U(\tau) \stackrel{\text{def}}{=} \Phi(x,y,\tau) + \mathrm{i}\Psi(x,y,\tau). \tag{11.11}$$

By this the equation of motion (11.5) can be written more simply as

$$\frac{\partial F}{\partial z}(z,\tau) = \frac{\partial w}{\partial \tau}(z,\tau) + \frac{\partial w}{\partial z}(z,\tau). \tag{11.12}$$

The Laplace transformation is defined by

$$\tilde{F}(z,s) = \int_0^\infty \mathrm{e}^{-s\tau} F(z,\tau)\,\mathrm{d}\tau, \quad s = s_1 + \mathrm{i}s_2, \quad s_1 > 0. \tag{11.13}$$

Application of this transformation to (11.12) yields

$$\frac{\partial \tilde{F}}{\partial z}(z,s) = \left(\frac{\partial}{\partial z} + s\right)\tilde{w}(z,s), \tag{11.14}$$

where it is assumed that the flexible plate starts moving at $t = \tau = 0$, whence $w(z,\tau) = u(x,y,\tau) - \mathrm{i}v(x,y,\tau) = 0$ for $\tau < 0$. Integrating (11.14) along a line $y = $ const. from $x = -\infty$ towards x, taking s real and considering the imaginary part of the result, we find

$$\tilde{\Psi}(x, y, s) = -\tilde{v}(x, y, s) - s \int_{-\infty}^{x} \tilde{v}(\xi, y, s)\, \mathrm{d}\xi. \tag{11.15}$$

This equation can be written as

$$\tilde{v}(x, y, s) = -\tilde{\Psi}(x, y, s) + s \int_{-\infty}^{x} \mathrm{e}^{s(\xi - x)} \tilde{\Psi}(\xi, y, s)\, \mathrm{d}\xi, \tag{11.16}$$

where the change from (11.15) to (11.16) follows from (11.14) by replacing $\partial/\partial z$ by $\partial/\partial x$ and solving $\tilde{v}$ from the imaginary part of the resulting equation.

Applying the Laplace transformation to (11.6), we have on the plate $\tilde{v}(x, 0, s) = \tilde{V}(x, s)$ and by (11.15) we find for $\tilde{\Psi}(x, 0, s)$ the relations

$$\tilde{\Psi}(x, \pm 0, s) = \mathfrak{Im}\, \tilde{F}(x \pm \mathrm{i}0, s) = \tilde{\Psi}_1(x, s) + \tilde{A}_0(s), \quad |x| < 1, \quad y = 0, \tag{11.17}$$

$$\tilde{\Psi}_1(x, s) = -\left(\frac{\partial}{\partial x} + s\right) \int_{-1}^{x} \tilde{V}(\xi, s)\, \mathrm{d}\xi, \quad |x| < 1, \quad y = 0, \tag{11.18}$$

$$\tilde{A}_0(s) = -s \int_{-\infty}^{-1} \tilde{v}(x, \pm 0, s)\, \mathrm{d}x = s \int_{-\infty}^{-1} \mathrm{e}^{s(x+1)} \tilde{\Psi}(x, 0, s)\, \mathrm{d}x. \tag{11.19}$$

The second equality in (11.19) follows by comparing (11.15) and (11.16) in which $x = -1$ and $y = 0$ have been taken. By (11.8) and (11.11) the 'pressure function' is found to be.

$$\tilde{\Phi}(x, \pm 0, s) = \mathfrak{Re}\, \tilde{F}(x \pm \mathrm{i}0, s) = 0, \quad |x| > 1. \tag{11.20}$$

Now the analysis of Wu has reached an important point. Equations (11.17) and (11.20), together with the conditions (11.9), can be written in the form of a Hilbert problem for the function $\tilde{F}(z, s) = \tilde{\Phi}(x, y, s) + \mathrm{i}\tilde{\Psi}(x, y, s)$, which is analytic in the whole $z = x + \mathrm{i}y$ plane, apart from a jump over the interval ($|x| < 1$, $y = 0$). Because $\varphi(x, y, t)$ is odd with respect to y (below (11.4)) also $\tilde{\Phi}(x, +0, s) = -\tilde{\Phi}(x, -0, s)$ and because $\mathfrak{Im}\, \tilde{F}(z, s) = \tilde{\Psi}(x, y, s)$ is known (11.17) at ($|x| < 1$, $y = 0$) except for the additive constant $\tilde{A}_0(s)$, we find

$$\tilde{F}^{+}(x, 0, s) = -\tilde{F}^{-}(x, 0, s) + 2\mathrm{i}\tilde{\Psi}(x, 0, s), \quad |x| < 1, \quad y = 0. \tag{11.21}$$

This is the Hilbert problem for the analytic function $\tilde{F}(z, s)$, the solution of which is given explicitly by Muskhelishvily in [21, p. 227 and further]. In fact, Wu formulates the problem as a Riemann–Hilbert problem, by demanding (11.17) and (11.20) along the + side of the whole real axis, hence for $z = x + \mathrm{i}0$.

The solution of problem (11.21) is

$$\tilde{F}(z, s) = \frac{1}{\pi \mathrm{i}} \left(\frac{z - 1}{z + 1}\right)^{1/2} \int_{-1}^{1} \left(\frac{1 + \xi}{1 - \xi}\right)^{1/2} \frac{\tilde{\Psi}(\xi, 0, s)}{(\xi - z)}\, \mathrm{d}\xi, \tag{11.22}$$

in which $\tilde{A}_0(s)$ (11.17) still has to be determined for which we refer to Wu's article. The square roots $(z - 1)^{1/2}$ and $(z + 1)^{1/2}$ are fixed by taking for each the positive square root for z real and $z > 1$, while there is a branch cut along the real axis from $z = -1$ to $z = 1$.

Now Wu applies the inverse Laplace transformation to (11.22). It can be asked if this is allowed because the analysis after (11.14) is based on the choice that s is real, while the inverse Laplace transformation needs an integration in the complex plane along a line parallel to the imaginary axis. However, this yields no difficulty, because it is known that Laplace transforms

are analytic with respect to s (11.13) and can be continued analytically from the real axis into the complex s plane.

In this way Wu arrives at a very complicated solution which we reproduce for the sake of completeness :

$$f(z,t) = \varphi(x,y,t) + \mathrm{i}\psi(x,y,t) = -\mathrm{i}U(t)\left\{A_0(\tau) - \tfrac{1}{2}a_0(\tau)\left(\frac{z-1}{z+1}\right)^{1/2}\right\} + \\ + \frac{1}{\pi i}\int_{-1}^{1}\left(\frac{z^2-1}{1-\xi^2}\right)^{1/2}\frac{\psi_1(\xi,t)}{(\xi-z)}\,\mathrm{d}\xi, \tag{11.23}$$

$$a_0(\tau) = -\int_0^{\tau}\{b_0(\tau') + b_1(\tau')\}H(\tau-\tau')\,\mathrm{d}\tau' + b_1(\tau), \tag{11.24}$$

$$b_n(\tau) = \frac{2}{\pi}\int_0^{\pi} V(x,t(\tau))\,\cos n\theta\,\mathrm{d}\theta, \quad (x = \cos\theta, n = 0,1,2\ldots), \tag{11.25}$$

$$H(\tau) = \frac{1}{2\pi\mathrm{i}}\int_{\epsilon-\mathrm{i}\infty}^{\epsilon+\mathrm{i}\infty}\mathrm{e}^{s\tau}\frac{K_1(s)}{K_0(s)+K_1(s)}\,\mathrm{d}s, \quad \epsilon > 0, \tag{11.26}$$

$$\psi_1(x,t) = -\left(\frac{\partial}{\partial t} + U(t)\frac{\partial}{\partial x}\right)\int_{-1}^{x} V(\xi,t)\,\mathrm{d}\xi, \tag{11.27}$$

$$A_0(\tau) = \frac{1}{2\pi\mathrm{i}}\int_{\epsilon-\mathrm{i}\infty}^{\epsilon+\mathrm{i}\infty}\{\tfrac{1}{2}\tilde{a}_0(s) - \frac{1}{\pi}\int_{-1}^{1}\tilde{\Psi}_1(\xi,s)(1-\xi^2)^{-1/2}\,\mathrm{d}\xi\}\,\mathrm{e}^{s\tau}\,\mathrm{d}s, \tag{11.28}$$

where $K_0(s)$ and $K_1(s)$ are modified Bessel functions of the second kind.

The suction force T_s at the nose is

$$T_s(\tau) = \tfrac{1}{2}\pi\rho\{\mathfrak{Re}\,a_0(\tau)\}^2. \tag{11.29}$$

From these results all physical quantities can be calculated, such as the jump of the pressure over the plate, the lift acting on the plate, the moment around some point acting on the plate, the thrust and the energy loss. For all these complicated formulas we refer to Wu's article [19, Part I].

We mention here also the article of Wu and Chwang 'Extraction of flow energy by fish and birds in a wavy stream' [24]. The authors consider the two-dimensional theory of a rigid profile moving in a wavy incoming stream for which the transverse velocities have the same frequency as that of the heaving and pitching motions of the profile. For a prescribed thrust (coefficient) C_{T_0} of the profile and a given amplitude $\tilde{\epsilon}$ of the incoming transverse velocity components, it is shown that a small contribution of the undesired leading-edge suction force occurs when the reduced frequency σ is in the neighbourhood of a calculated σ_m, which is a function of C_{T_0} and $\tilde{\epsilon}$.

12. Existence of optimum propulsion. Flat plate, two-dimensional theory

The two-dimensional linearized hydrodynamics of the thrust production by a flat plate carrying out a purely harmonic motion that consists of combined heaving and pitching in a parallel

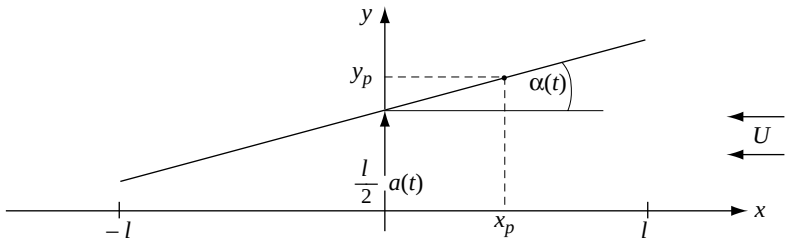

Figure 20. Rigid flat plate in uniform parallel flow.

flow with a time-independent velocity is clearly a special case of Wu's general theory that we discussed in the previous section. This special case was discussed by Lighthill [14] and, very comprehensively, by Wu [19, Part 2].

Lighthill and Wu considered the propulsion by means of a rigid plate as a tool to obtain insight in the hydrodynamics of the carangiform of swimming of, for instance, cetaceans with a lunate tail. In fact, this theory can be used for a strip theory of a wing of relatively large aspect ratio such as the lunate sail.

Both mentioned authors start by choosing a purely harmonic motion and for a given frequency discuss the influence of the amplitudes of the heaving and pitching parts of the motion and of their phase difference on the efficiency of the propulsion. An interesting point is also to what extent the suction force contributes to the total thrust, because this force can induce flow separation at the nose of the plate. Wu gives results about the quotient of the mean value of the suction force and the total mean thrust in order to be able to decide if a certain thrust production is reliable with respect to leading-edge stall.

However, in this section and the following one we will try to give an impression of the work of H.P. Urbach, which is partly based on the older work of Lighthill and Wu. We start with his article 'Existence of optimum propulsion by means of periodic motions of a rigid profile' [25]. This more recent work is rather advanced in that it uses functional analysis and it seems interesting to get in touch with results that can be obtained by means of methods that may yield farther reaching results than are possible by classical applied mathematics. Urbach proves among other things that the purely harmonic motion, as assumed by Lighthill and Wu, is the optimum motion in comparison with other periodic motions from a large class of admitted ones. The dangerous suction force is kept in check by him by prescribing in advance its tolerated contribution to the thrust.

The periodic motion of the plate is assumed to be of the form (Figure 20)

$$y = h(x,t) = \frac{l}{2}a(t) + \alpha(t)x = O(\epsilon), \quad -l \le x \le l, \tag{12.1}$$

where ϵ is again a small parameter used for linearization, $2l$ is the length of the plate and the dimensionless functions $a(t)$ and $\alpha(t)$ determine the heaving and the pitching of the plate. The plate is placed in a uniform parallel flow of velocity U in the negative x-direction.

The mean value of the total thrust which depends on $h(x,t)$ is denoted by $T(h)$ and the mean value of the suction force by $T_s(h)$. The mean value of the lost kinetic energy per second is $E(h)$. Then the efficiency of the propulsion becomes

$$\eta(h) = \frac{UT(h)}{UT(h) + E(h)}. \tag{12.2}$$

The point (x_p, y_p) can be thought of as the point at which the plate is clutched and forced to carry out the motion $y = h(x, t)$ and can be used to put a constraint on the amplitude of the plate, $|h(x_p, t)| \leq C$. This point may also be situated at the extension of the plate $|x_p| > l$. The chosen period of motion is τ_0 and the demanded mean thrust is T_0. The quotient of the mean suction force T_s and the demanded mean thrust is $r = T_s(h)/T_0$.

The optimization problem (P) has then, in first instance, the following crude form

$$(P): \text{Minimize } E(h), \text{ subject to } h \in A, \tag{12.3}$$

$$\begin{aligned} A = \{h : h(x, t + \tau_0) = h(x, t)\ \forall t, \quad T(h) = T_0, \quad T_s(h) \leq rT_0 \quad (0 \leq r < \infty), \\ \max_t |h(x_p, t)| \leq C, \quad 0 \leq C \leq \infty\}, \end{aligned} \tag{12.4}$$

where r and C are fixed numbers. When $C = \infty$ there is no constraint on the amplitude of the motion. We note that in the condition on r, which yields the announced check on the suction force, namely $0 \leq r < \infty$, the inequality $< \infty$ is essential; hence r has to be finite (see below (13.13)).

The functions $a(t)$ and $\alpha(t)$ that determine $h(x, t)$ (12.1) will have the representation

$$a(t) = \sum_{m=-\infty}^{\infty} \hat{a}(m) \mathrm{e}^{\mathrm{i}m\omega_0 t}, \quad \hat{a}(m) = \frac{1}{\tau_0} \int_0^{\tau_0} a(t) \mathrm{e}^{-\mathrm{i}m\omega_0 t}\, \mathrm{d}t, \tag{12.5}$$

$$\alpha(t) = \sum_{m=-\infty}^{\infty} \hat{\alpha}(m) \mathrm{e}^{\mathrm{i}m\omega_0 t}, \quad \hat{\alpha}(m) = \frac{1}{\tau_0} \int_0^{\tau_0} \alpha(t) \mathrm{e}^{-im\omega_0 t}\, \mathrm{d}t, \tag{12.6}$$

$$\omega_0 = 2\pi/\tau_0, \quad \hat{a}(-m) = \overline{\hat{a}(m)}, \quad \hat{\alpha}(-m) = \overline{\hat{\alpha}(m)}, \tag{12.7}$$

where $a(t)$ and $\alpha(t)$ are real and a bar denotes complex conjugated values.

Because there are infinitely many coefficients $\hat{a}(m)$ and $\hat{\alpha}(m)$, this problem is infinite-dimensional as contrasted with the rigid-plate problem discussed by Lighthill and Wu, where by the choice of a purely harmonic motion the problem was finite-dimensional. So here an existence proof is appropriate.

Now the formulation of the optimization problem (P) will be sharpened. First, the well-known dimensionless coefficients

$$C_T(h) = \frac{4T(h)}{\pi\rho U^2 l}, \quad C_{T_s}(h) = \frac{4T_s(h)}{\pi\rho U^2 l}, \quad C_E(h) = \frac{4E(h)}{\pi\rho U^3 l}, \quad \eta(h) = \frac{C_T}{C_T + C_E}. \tag{12.8}$$

are introduced. Because $h(x, t)$ is determined by $a(t)$ and $\alpha(t)$, a function space has to be chosen for the admitted functions $a(t)$ and $\alpha(t)$. The function space that Urbach shows to be suitable for this purpose is the Hilbert space $H^1_{\tau_0}$ consisting of functions that are periodic with period τ_0, absolutely continuous and whose derivative is square Lebesque integrable.

It can be proved that the first three coefficients defined in (12.8) depend only on the reduced frequency $\sigma_0 = \omega_0 l/U$ and on the Fourier coefficients of $a(t)$ (12.5) and $\alpha(t)$ (12.6). Then, for given σ_0, C_{T_0}, r and C_∞ with $0 < C_{T_0} < \infty, 0 \leq r < \infty, 0 < C_\infty \leq \infty$ and for x_p with $|x_p| < \infty$, the optimization problem is reformulated as

$$(P): \text{Minimize } C_E(a, \alpha), \text{ subject to } (a, \alpha) \in A, \tag{12.9}$$

$$A = \left\{(a,\alpha) \in H^1_{\tau_0} \times H^1_{\tau_0};\quad C_T(a,\alpha) = C_{T_0}, C_{T_s}(a,\alpha) \le rC_{T_0}, ||\tfrac{1}{2}a + \frac{\alpha x_p}{l}||_\infty \le C_\infty\right\}, \tag{12.10}$$

where $\|\frac{1}{2}a + \alpha x_p/l\|_\infty = \max|\frac{1}{2}a(t) + \alpha(t)x_p/l|$ for $0 \le t \le \tau_0$ and where, instead of the dependence on h of the coefficients (12.8), their dependence on (a,α) is denoted. The quantities $C_E(a,\alpha)$, $C_T(a,\alpha)$ and $C_{T_s}(a,\alpha)$ are quadratic functionals of (a,α) that can be calculated as a special case of Wu's theory outlined in the previous section.

There exists a transformation of variables from the functions $a(t)$ and $\alpha(t)$ to new functions $z(t)$ and $\zeta(t)$ such that, when written in terms of these new functions, two of the three quadratic functionals become diagonalized. The transformation is given by

$$z(t) = \sum_{m=-\infty}^{\infty} \hat{z}(m)\mathrm{e}^{\mathrm{i}m\omega_0 t}, \quad \zeta(t) = \sum_{m=-\infty}^{\infty} \hat{\zeta}(m)\mathrm{e}^{\mathrm{i}m\omega_0 t}, \quad \hat{z}(-m) = \overline{\hat{z}(m)}, \quad \hat{\zeta}(-m) = \overline{\hat{\zeta}(m)}, \tag{12.11}$$

$$\hat{z}(0) = \hat{a}(0), \quad \hat{\zeta}(0) = \hat{\alpha}(0), \tag{12.12}$$

$$\begin{pmatrix} \hat{z}(m) \\ \hat{\zeta}(m) \end{pmatrix} = \begin{pmatrix} B(m\sigma_0)^{1/2} & \left(-1 + \dfrac{2\mathrm{i}}{m\sigma_0}\right) B(m\sigma_0)^{1/2} \\ T_{11}(m\sigma_0)^{1/2} & \left(-1 + \dfrac{2\mathrm{i}}{m\sigma_0}\right) T_{11}(m\sigma_0)^{1/2} \end{pmatrix} \begin{pmatrix} \hat{a}(m) \\ \hat{\alpha}(m) \end{pmatrix}, \quad m \ne 0. \tag{12.13}$$

We do not give $B(\sigma)$ and $T_{11}(\sigma)$ but only mention that they depend on Theodorsen's function

$$\Theta(\sigma) = \frac{H_1^{(2)}(\sigma)}{H_1^{(2)}(\sigma) + \mathrm{i}H_0^{(2)}(\sigma)}, \quad \sigma > 0, \tag{12.14}$$

where $H_m^{(2)}(\sigma)$ are Hankel functions of the second type.

Then it turns out that the first three coefficients of (12.8) become

$$C_E(z) = \sum_{m=-\infty}^{\infty} 2m^2\sigma_0^2|\hat{z}(m)|^2, \tag{12.15}$$

$$C_T(z,\zeta) = C_E(z) + \sum_{m=-\infty}^{m} 4m^2\sigma_0^2\tilde{T}_{12}(m\sigma_0)\overline{\hat{z}(m)}\hat{\zeta}(m) \stackrel{\text{def}}{=} C_E(z) + R_T(z,\zeta), \tag{12.16}$$

$$C_{T_s}(\zeta) = 8|\hat{\zeta}(0)|^2 + \sum_{m=-\infty}^{\infty} 2m^2\sigma_0^2|\hat{\zeta}(m)|^2, \tag{12.17}$$

$$\tilde{T}_{12}(\sigma) = -\frac{1}{2}\frac{\Theta(\sigma)}{B(\sigma)^{1/2}T_{11}(\sigma)^{1/2}} + \left(1 - \frac{\mathrm{i}}{\sigma}\right)\frac{T_{11}(\sigma)^{1/2}}{B(\sigma)^{1/2}}. \tag{12.18}$$

It follows from (12.17) that, when $C_{T_s}(\zeta) = 0$, and hence, when the suction force is zero for each t because it is a positive quantity, then $\zeta(t) = 0$ since all its Fourier coefficients have to be zero. Then, by (12.16) $C_T(z,0) = C_E(z)$ and the following interesting result is found

$$\boxed{\eta(h) = \frac{C_T(h)}{C_T(h) + C_E(h)} = \frac{1}{2}, \quad r = 0}, \tag{12.19}$$

which was not obtained in previous articles.

By using the new variables (z, ζ) instead of (a, α) (12.11) and (12.12), Urbach remoulds the minimizing problem (P) (12.9) and (12.10) into a number of other forms from which he finds after a complicated analysis, for which we refer to his paper, the final existence theorem. We quote

THEOREM

For every $\sigma_0, C_{T_0}, r, C_\infty$ with $0 < C_{T_0} < \infty, 0 \leq r < \infty, 0 < C_\infty$ and for every point (x_p, y_p), there exists at least one solution of problem (P). For fixed σ_0, r, C_∞ and x_p, the efficiency of the solution is non-increasing when the required mean thrust C_{T_0} is increasing. Furthermore, all motions for which the suction force at the nose of the plate vanishes at all times have efficiency $\frac{1}{2}$, so that problem (P) is trivial for $r = 0$.

In this theorem nothing is said about the uniqueness of the solution of the optimization problem; for instance, from every solution an other solution can be obtained by means of an equal phase shift in $a(t)$ and $\alpha(t)$, but it is not excluded that there are also other solutions with a more profound difference.

If, in the theorem, the case $C_\infty = 0$ is excluded from the admitted interval of C_∞, then only pitching motions of the plate can occur around the point $(x_p, 0)$. This causes some difficulties, because it can then be proved that not all values of r in the interval $0 \leq r < \infty$ can be used. Also, the case $r = \infty$ is excluded, since in the next section we will discuss that for $r = \infty$ no optimum motion can exist; see below (13.13).

13. Optimum propulsion. Flat plate, two-dimensional theory

We follow again Urbach, but now in his paper 'On optimum propulsion by means of small periodic motions of a rigid profile, I. Properties of optimum motions' [26]. We consider mainly the case that in the optimization problem (P), given by (12.9) and (12.10), the constraint on the amplitude of the point (x_p, y_p) is removed by taking $C_\infty = \infty$.

The optimization problem expressed in the new variables $z(t)$ and $\zeta(t)$ (12.12) and (12.13) is now formulated as

$$(\tilde{P}) : \text{Minimize } C_E(z) \text{ subject to } z \in A_1, \tag{13.1}$$

$$A_1 = \{z \in H^1_{\tau_0}, \text{there exist } \zeta \in H^1_{\tau_0} \text{ such that } C_T(z, \zeta) \geq C_{T_0}, C_{T_s}(\zeta) \leq r C_{T_0}\}. \tag{13.2}$$

The definition of the function space A_1 is different from the function space A in (12.10); instead of $C_T(a, \alpha) = C_{T_0}$ the inequality $C_T(z, \zeta) \geq C_{T_0}$ (desired shrust coefficient) is imposed. This, however, yields the same solution of the optimization problem because the existence theorem of the previous section states that the efficiency η is non-increasing with increasing C_T; hence by (12.8) C_E is increasing with C_T. By this the minimum of C_E occurs also for $C_T = C_{T_0}$.

The advantage of the new formulation (13.2) is that only inequality conditions appear in problem $(\tilde{P})$, so that the Kuhn–Tucker theorem can be applied. For the Kuhn–Tucker problem see for instance the clear discussion by Luenberger in his book 'Optimization by vector space methods' [27]. For this the Gateaux derivative of a functional is used, namely for C_E (12.15)

$$\delta C_E(z_0)(z) = \lim_{\epsilon \to 0} \frac{1}{\epsilon}\{C_E(z_0 + \epsilon z) - C_E(z_0)\} = \sum_{m=-\infty}^{\infty} 4m^2\sigma_0^2 \hat{z}_0(m)\overline{\hat{z}(m)}, \tag{13.3}$$

where the derivative is at z_0, z is arbitrary and $\hat{z}(m) = \overline{\hat{z}(-m)}$. Analogously, from (12.16) and (12.17)

$$\begin{aligned}\delta C_T(z_0,\zeta_0)(z,\zeta) = \ & \delta C_E(z_0)z + \sum_{m=-\infty}^{\infty} 4m^2\sigma_0^2\{\tilde{T}_{12}(m\sigma_0)\hat{z}_0(m)\overline{\hat{\zeta}(m)} + \\ & + \tilde{T}_{12}(m\sigma_0)\overline{\hat{z}(m)}\hat{\zeta}_0(m)\},\end{aligned} \tag{13.4}$$

$$\delta C_{T_s}(\zeta_0)(\zeta) = 16\hat{\zeta}_0(0)\hat{\zeta}(0) + \sum_{m=-\infty}^{\infty} 4m^2\sigma_0^2\hat{\zeta}_0(m)\overline{\hat{\zeta}(m)}, \tag{13.5}$$

with $\hat{\zeta}(m) = \overline{\hat{\zeta}(-m)}$.

In order to be able to apply the Kuhn–Tucker theorem, Urbach shows that the two inequality conditions in (13.2) satisfy certain regularity conditions. Then the Kuhn–Tucker theorem states that, when z_0 is a solution that minimizes $C_E(z)$ and when (z_0, ζ_0) satisfy the conditions for (z, ζ) in (13.2), there exist Lagrange multipliers $\lambda_1 \geq 0$ and $\lambda_2 \geq 0$ such that for every $(z, \zeta) \in H^1_{\tau_0} \times H^1_{\tau_0}$

$$\delta C_E(z_0)(z) - \lambda_1\delta C_T(z_0,\zeta_0)(z,\zeta) + \lambda_2\delta C_{T_s}(\zeta_0)(\zeta) = 0, \tag{13.6}$$

$$\lambda_1\{C_T(z_0,\zeta_0) - C_{T_0}\} = 0, \quad \lambda_2\{C_{T_s}(\zeta_0) - rC_{T_0}\} = 0. \tag{13.7}$$

Because z and ζ are arbitrary, it follows from (13.3)–(13.5) that (13.6) is equivalent to

$$\lambda_2\hat{\zeta}_0(0) = 0, \tag{13.8}$$

$$(1-\lambda_1)\hat{z}_0(m) - \lambda_1\tilde{T}_{12}(m\sigma_0)\hat{\zeta}_0(m) = 0, \ m = 1, 2, \ldots, \tag{13.9}$$

$$-\lambda_1\overline{\tilde{T}_{12}(m\sigma_0)}\hat{z}_0(m) + \lambda_2\hat{\zeta}_0(m) = 0, \quad m = 1, 2, \ldots. \tag{13.10}$$

It can be proved that $|\tilde{T}_{12}(\sigma)|^2$ is an even function which decreases monotonically with increasing $\sigma = \omega l/U$. In addition, it holds that $\lim_{\sigma\to 0}|\tilde{T}_{12}(\sigma)|^2 = \infty$ and $\lim_{\sigma\to\infty}\sigma^2|\tilde{T}_{12}(\sigma)|^2 = 9/16$.

Hence $\tilde{T}_{12}(m\sigma) \neq 0$ for every m and from this it follows that $\lambda_2 > 0$. Indeed, suppose that $\lambda_2 = 0$. Then by (13.9) and (13.10), because $\lambda_1 \geq 0$, we have $\tilde{z}_0(m) = 0$ for $m = 1, 2, \ldots$. Then by (12.15) and (12.16) $C_T(z_0, \zeta_0) = 0$, which contradicts (13.2). So $\lambda_2 > 0$ and then by (13.8)

$$\hat{\zeta}_0(0) = 0. \tag{13.11}$$

Because $\hat{z}(0)$ does not appear in C_E, C_T and C_{T_s} we may put

$$\hat{z}_0(0) = 0. \tag{13.12}$$

The fact that $\lambda_2 > 0$ yields another interesting result, namely it follows from the second equation of (13.7) that

$$\boxed{C_{T_s}(\zeta_0) = rC_{T_0}}. \tag{13.13}$$

Hence the maximum admitted suction force occurs in the optimum motion. This is the reason that it has to be demanded that $r < \infty$, otherwise the mean suction force becomes ∞ and there does not exist a suitable optimum motion.

By (13.9) it is seen that, if $\lambda_1 = 0$, then $\hat{z}_0(m) = 0$ for $m = 1, 2, \ldots$, which is not allowed as we remarked above (13.11); hence $\lambda_1 > 0$. Because (13.9) and (13.10) are two homogeneous equations for $\hat{z}_0(m)$ and $\hat{\zeta}_0(m)$, the determinant of these equations has to be zero, or

$$\frac{(1-\lambda_1)\lambda_2}{\lambda_1^2} = |\tilde{T}_{12}(m\sigma_0)|^2. \tag{13.14}$$

The existence theorem in the previous section states that there is at least one optimum solution of the problem, while it follows from the mentioned monotony of $|T_{12}(m\sigma_0)|^2$ that there is at most one m for which (13.14) holds. Because $\hat{\zeta}_0(0) = \hat{z}_0(0) = 0$, (13.11) and (13.12), it is found that the optimum $z_0(t)$ and $\zeta_0(t)$ are purely harmonic functions with the same frequency, or

$$z_0(t) = 2\,\mathfrak{Re}\,(\hat{z_0}(m)\mathrm{e}^{\mathrm{i}m\omega_0 t}), \quad \zeta_0(t) = 2\,\mathfrak{Re}\,(\hat{\zeta_0}(m)\mathrm{e}^{\mathrm{i}m\omega_0 t}), \tag{13.15}$$

for some value of m.

Then by (12.15)–(12.17) and (13.13) it is found that

$$C_E(z_0) = 4m^2\sigma_0^2|\hat{z}_0(m)|^2, \tag{13.16}$$

$$C_T(z_0) = 4m^2\sigma_0^2\{|\hat{z}_0(m) + \tilde{T}_{12}(m\sigma_0)\hat{\zeta}_0(m)|^2 - |\tilde{T}_{12}(m\sigma_0)|^2|\hat{\zeta}_0(m)|^2\}, \tag{13.17}$$

$$C_{T_s}(\zeta_0) = 4m^2\sigma_0^2|\hat{\zeta}_0(m)|^2 = rC_{T_0}. \tag{13.18}$$

Because the phase of the motion is not of interest, $\hat{\zeta}_0(m)$ can be taken real and positive in (13.18):

$$\hat{\zeta}_0(m) = \frac{(rC_{T_0})^{1/2}}{2m\sigma_0}. \tag{13.19}$$

Hence, when m is considered to be fixed, it follows from (13.16) and (13.17) that $\hat{z}_0(m)$ has to be the solution of the following optimization problem:

($\tilde{P}$) : Minimize $|z|^2$, where z is a complex number for which by (13.17) the following holds

$$|z + \tilde{T}_{12}(m\sigma_0)\hat{\zeta}_0(m)|^2 = \frac{C_{T_0}}{4m^2\sigma_0^2} + |\tilde{T}_{12}(m\sigma_0)|^2|\hat{\zeta}_0(m)|^2. \tag{13.20}$$

From this it is found that

$$\hat{z}_0(m) = \left\{\left(1 + \frac{C_{T_0}}{|\tilde{T}_{12}(m\sigma_0)|^2|\hat{\zeta}_0(m)|^2}\right)^{1/2} - 1\right\}\tilde{T}_{12}(m\sigma_0)\hat{\zeta}_0(m). \tag{13.21}$$

From (13.19) the corresponding rate-of-energy loss becomes

$$C_E(z_0) = \left[\{r|\tilde{T}_{12}(m\sigma_0)|^2 + 1\}^{1/2} - r^{1/2}|\tilde{T}_{12}(m\sigma_0)|\right]^2 C_{T_0}. \tag{13.22}$$

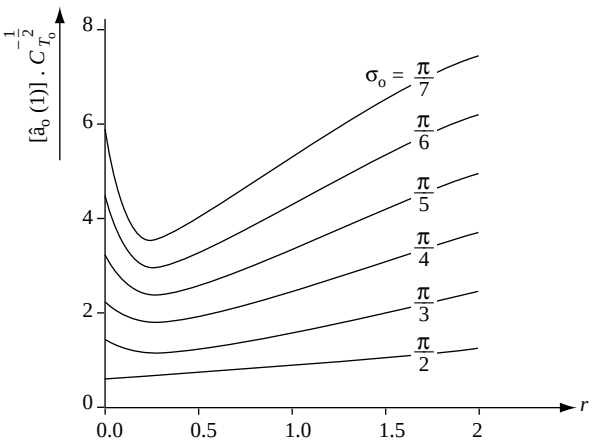

Figure 21. $|\hat{a}_0(1)|C_{T_0}^{-\frac{1}{2}}$ as a function of r (12.4) for several values of σ_0. From Urbach [26].

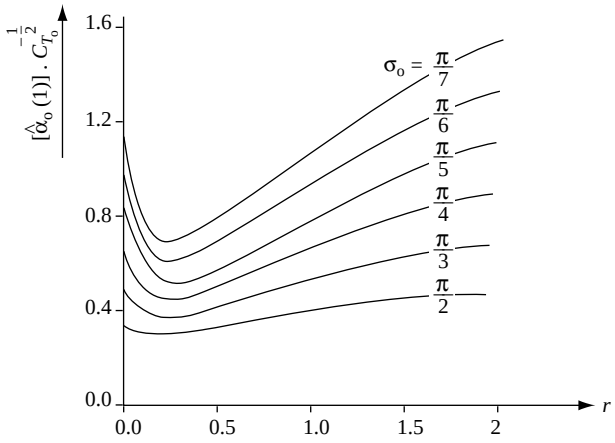

Figure 22. $|\hat{\alpha}_0(1)|C_{T_0}^{-\frac{1}{2}}$ as a function of r (12.4) for several values of σ_0. From Urbach [26].

By the mentioned monotony property of $|\tilde{T}_{12}(m\sigma_0)|^2$ it follows that $C_E(z_0)$ assumes its minimum for $m = 1$.

Using the inverse transformation of (12.12) and (12.13) and some manipulations, Urbach has found for the optimum motion the form

$$y = h_0(x,t) = l|\hat{a}_0(1)| \sin\, \omega_0 t + 2x|\hat{\alpha}_0(1)| \sin(\omega_0 t + \varphi)\,. \tag{13.23}$$

The amplitudes $|\hat{a}_0(1)|$ and $|\hat{\alpha}_0(1)|$, as well as the phase φ, in this formula are given in Figures 21–23 as functions of σ and r, respectively

The efficiency η of the optimum motion is given in Figure 24. As we discussed in Section 2 below (2.16), this efficiency is independent of the desired thrust or independent of C_{T_0}.

The phase difference between the heaving and pitching parts of the motion depends on the choice of the position of the pitching axis, which is at $x = 0$ in (13.23). Applying a shift in time $t \to t - \varphi/\omega$, we find for (13.23)

$$y = h_0(x,t) = -l|\hat{a}_0(1)| \cdot \sin\, \varphi\, \cos\, \omega_0 t + 2|\hat{\alpha}_0(1)| \left\{ x + \frac{l|\hat{a}_0(1)|}{2|\hat{\alpha}_0(1)|} \cos\, \varphi \right\} \sin\, \omega_0\, t,$$

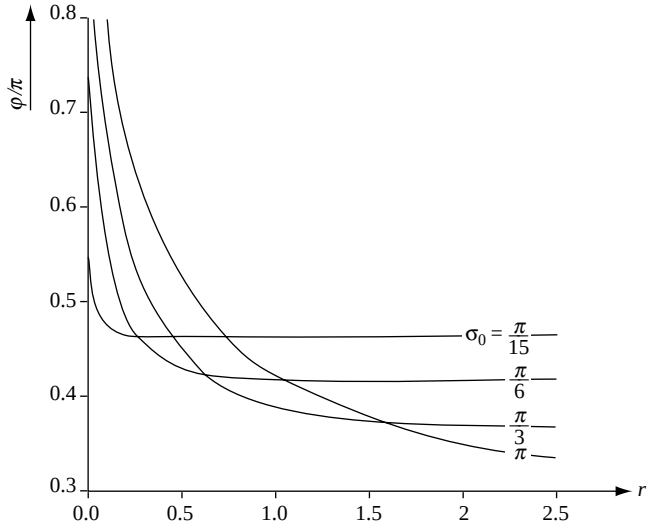

Figure 23. φ as a function of r (12.4) for several values of σ_0. From Urbach [26].

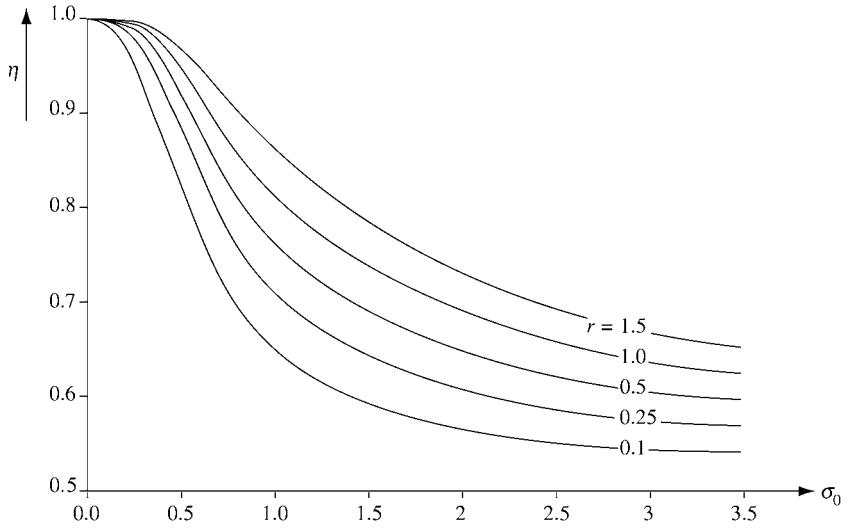

Figure 24. η as a function of σ_0 for several values of r (12.4). From Urbach [26].

(13.24)

where this phase difference is $\frac{1}{2}\pi$, which is constant, but now the pitching axis, which we denote by $x = x^* = -\frac{1}{2}l|\hat{a}_0(1)| \cdot |\hat{\alpha}_0(1)|^{-1} \cos\varphi$, is variable. Next we discuss the concept of feathering which was introduced by Lighthill in 'Hydromechanics of aquatic propulsion: a survey' [28]. This concept is coupled to the description of the plate motion (13.24) with the constant phase difference $\frac{1}{2}\pi$ between heaving and pitching. The angle β_1 between plate and x-axis and the slope β_2 of the trajectory through the fluid of the pitching axis, which is represented by the point Q defined by

$$Q = \left(-\frac{l|\hat{a}_0(1)|}{2|\hat{\alpha}_0(1)|} \cos\varphi, \quad -l|\hat{a}_0(1)| \sin\varphi \cos\omega_0 t \right), \tag{13.25}$$

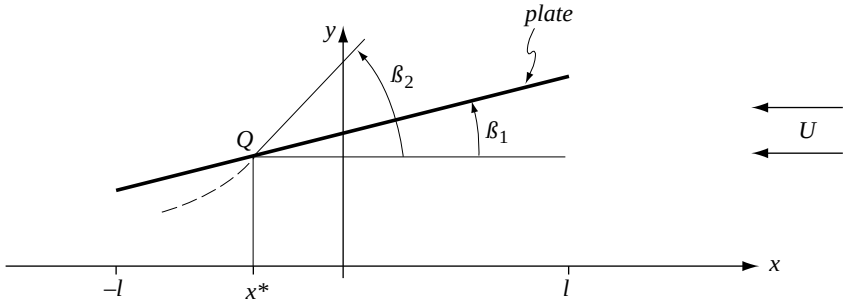

Figure 25. Feathering $F = \beta_1/\beta_2$,- - - - trajectory of Q with respect to fluid.

Table 1.

σ_0	0·1		0·5				r
$\pi/6$	$x^* = 0{\cdot}32l$	$F = 0{\cdot}77$	$\eta = 0{\cdot}77$	$x^* = -0{\cdot}53l$	$F = 0{\cdot}84$	$\eta = 0{\cdot}92$	
$\pi/3$	$x^* = 0{\cdot}66l$	$F = 0{\cdot}65$	$\eta = 0{\cdot}63$	$x^* = -0{\cdot}31l$	$F = 0{\cdot}63$	$\eta = 0{\cdot}75$	

are (Figure 25) given by

$$\beta_1 = \frac{\partial y}{\partial x} = 2|\hat{\alpha}_0(1)| \sin \omega_0 t, \quad \beta_2 = \frac{1}{U}\frac{\partial y}{\partial t} = \frac{l\omega_0}{U}|\hat{a}_0(1)| \sin \varphi \cos \omega_0 t, \tag{13.26}$$

respectively. Then the feathering is defined by

$$F = \frac{\beta_1}{\beta_2} = \frac{2|\hat{\alpha}_0(1)|}{\sigma_0|\hat{a}_0(1)|}, \tag{13.27}$$

which will be smaller than 1 in the case of good propulsion, which follows from Figure 25, where Q has to move upwards sufficiently fast in order that the plate yields a thrust in the positive x-direction.

Using Figures 21–23 we can determine from (13.24) the location $x = x^*$ of the pitching axis for a phase difference of $\frac{1}{2}\pi$ between heaving and pitching, from (13.27) the feathering F and from Figure 24 the efficiency η. This is carried out for $\sigma_0 = \pi/6$ and $\sigma_0 = \pi/3$ and for $r = 0{\cdot}1$ and $r = 0{\cdot}5$. We remark that, because we have measured the values of $|\hat{a}_0(1)|$, $|\hat{\alpha}_0(1)|$ and φ from the graphs, the results will not be very accurate; however, some insight can be gained from them; see Table 1.

The advantage of the theory of Urbach is that for each given pair $\sigma_0 = \omega_0 l/U$ and r, the position of the pitching axis for the representation (13.24) of the motion is uniquely determined in case of the optimum motion. It follows from the table that, for larger values of r ($r = 0{\cdot}5$), hence for a larger contribution of the suction force at the leading edge of the plate, the pitching axis is situated at the rear half of the plate, while for smaller values of r ($r = 0{\cdot}1$) the pitching axis is at the front part of the plate, both in the case of optimum motions. These results can possibly add to the results obtained by Lighthill [13] and Wu [19, Part 2], who both come to the conclusion that the 'best' region of the pitching axis in (13.24) is somewhere between the 3/4 chord point and the trailing edge or $-l < x^* < -0{\cdot}5l$. It seems desirable to have more results based on Urbach's theory than the four listed in Table 1.

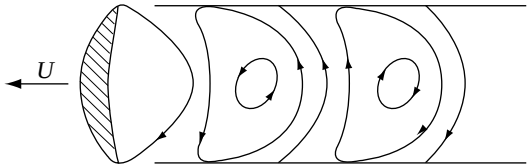

Figure 26. Lunate tail (hatched region), with shed vorticity. From Chopra and Kambe [29].

For more information about the optimum propulsion by means of the rigid plate we refer to Urbach [26]. Among other things, he discusses the influence of a constraint on the amplitude of the motion of point (x_p, y_p) (Figure 20) which, as we mentioned before, is an arbitrary point on the plate where it can be forced to carry out a desired motion. This constraint is formulated in (12.10) by means of a chosen finite value of C_∞. When the demanded thrust coefficient is sufficiently high, this constraint becomes active and a purely harmonic optimum motion is in general impossible; then the heaving and pitching motions have infinitely many non-zero Fourier coefficients, which complicates the analysis considerably. It is shown by Urbach that the trajectory of (x_p, y_p) then reaches smoothly its maximum $y = C_\infty$, retains this value some time until it leaves smoothly $y = C_\infty$ and crosses over smoothly to its limit at the other side.

When, $C_\infty < \infty$, it is also possible to optimize the reduced frequency σ; this is discussed at the end of [26, Part II]. It is perhaps interesting to investigate if this has some bearing on the frequency σ used by fishes when they have by their structural constellation some, be it not rigorously fixed, maximum value of the amplitude of their tail motion.

14. Different types of research on caudal-fin propulsion

Up to now we have discussed mainly two hydrodynamic theories, namely slender-body theory and the two-dimensional theory of the waving plate. These two theories are based on elegant mathematical considerations and by this give insight in the influence of some important parameters. However, it is also of interest to consider more specific hydrodynamic problems, for instance, the propulsion by a lunate tail. As is remarked by Lighthill, this type of tail is found in such distinct aquatic animals as fast sharks and cetacean mammals which clearly came to this form along different paths in their evolution. Because of its large aspect ratio, the first approximation of such a tail is afforded by the two-dimensional theory of the waving plate. However, its finite span, its sweep back and its tapered shape are neglected.

Chopra and Kambe in their 'Hydrodynamics of lunate tail swimming propulsion, Part 2' [29] have calculated, by means of a lifting-surface theory for several flat lunate tails, values of reduced frequency, positions of the pitching axis and feathering parameters, the thrust coefficient and the efficiency. For the specific values of the parameters we refer to the article. From the many numerical results they found two general properties which we mention here. First, a smoothly and not too strongly bent leading edge diminishes the contribution of the suction force to the total thrust without loss of efficiency and hence delays flow separation at the leading edge. Second, they found that, for some fixed reasonable value of the thrust coefficient, the parameter values for maximum efficiency are such that no negative hydrodynamical work is done in the oscillation of the tail. The latter is important because, as we quote, 'biologists have shown that positive energy is incrusted in the musculature not only when animals do positive work but also when they do negative work', which yields an efficiency lower than the hydrodynamical efficiency.

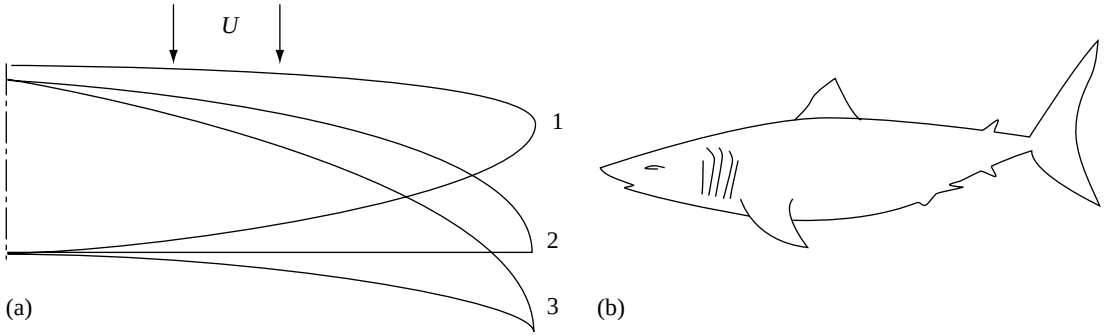

Figure 27. (a) The considered three wing planforms, (b) *Isurus oxyrinchus* with lunate tail. Based on van Dam [31].

The shed vorticity drawn in Figure 26 belongs to a lunate tail motion with good efficiency, at the moment when the tail is in the plane of drawing and is moving downwards.

We also mention Karpouzian, Spedding and Cheng 'Lunate tail swimming propulsion, Part 2. Performance analysis' [30]. From their numerical results they draw the following two general conclusions:

First, an increase in the heaving of the peduncle (connection of tail and body) decreases the value of the optimum sweep back until the latter becomes zero. Second, we quote: 'if one postulates a tendency in carangiform evolution towards increasingly restricted motion of the caudal peduncle, in the interests of reducing wake-energy losses, for example, then the increase in sweep angle of the tail appears a design option to compensate for the reduced peduncle heaving amplitude'. Both conclusions are apparently related.

Finally, with respect to the lunate tail, we mention the work of van Dam 'Efficiency characteristics of crescent wings and caudal fins' [31], who made calculations of the induced resistance of wings with the shape of a lunate tail in steady flow. The calculations by means of surface panels (1000) on the wing and on part of the wake simulate the vortex roll-up at the tips of the wings. The author defines the 'induced efficiency' e by

$$D_i = 2L^2/(\pi\rho U^2 b^2 e), \tag{14.1}$$

where D_i is the induced drag, L denotes the lift, b is the span of the wing and U is the free-stream velocity.

Three types of wings are considered (Figure 27a), all with the same aspect ratio $b^2/S = 7$, where S is the area of the planform, *viz.*, (1) elliptical wing with straight quarter chord line, (2) wing with straight trailing edge, (3) wing with typical crescent shape, all having the same spanwise chord distribution. Each wing has the symmetrical NACA 0012 section shape in the streamwise direction. The wings are placed under an angle of incidence $\alpha = 4°$. Then the numbers e have the values (1) $e = 1{\cdot}000$, (2) $e = 1{\cdot}045$ and (3) $e = 1{\cdot}088$ which clearly show a favourable property of the steady lunate tail which, as the author states, will manifest itself also in case of unsteady propulsion when the reduced frequency $\sigma = \omega c_{av}/U < 0{\cdot}6$, where ω is the radian frequency and c_{av} the meanchord.

The results of van Dam mentioned above differ from the results found by Ashenberg and Weihs in their papers 'Curved lifting line theory for thin planar wings' [32] and 'Minimum induced drag of wings with curved planform' [33]. These papers use Prandtl's lifting-line theory adapted to curved planforms (that are flat). They do not predict an improved aerodynamic

efficiency for crescent-shaped planforms. So it seems that the nonlinear approach given in [31] is needed for the understanding of the efficacy of the lunate tail.

We now mention the paper by Cheng, Zhuang and Tong entitled 'Analysis of swimming three-dimensional waving plates' [34] which considers numerically the swimming of a flexible rectangular plate of finite span, hence it partly shows to which extent the analytical two-dimensional theory of Wu (Section 11) is valid for finite span. The considered plate has chord-length 1, the incoming velocity in the x-direction is given by $U = 1$. The prescribed motion of the plate has the form $h(x, t) = x^m \cos(\omega t - kx)$, where $m = 0,1,2$ or 3, $\omega = 8$ and $-3 \leq k \leq 7$. One of the remarkable results is then that the efficiencies of these swimming plate motions are only very weakly dependent on the aspect ratio A which are considered for $A = 0{\cdot}5$, $A = 1$ and $A = 8{\cdot}5$. The dependency is increasing somewhat with m, where for $m = 3$, contrary to expectation, the efficiency is slightly decreasing with increasing values of A.

Katz and Weihs, in their 'Hydrodynamic propulsion by large amplitude oscillation of an airfoil with chordwise flexibility' [35] study the two-dimensional case of a propelling plate carrying out a large-amplitude motion, governed by the translation and rotation of the leading edge, in such a way that the induced velocities are small. The plate is flexible and bends passively under the influence of pressures, while its wake moves in concurrence with the induced velocities.

It is shown, for a rigid plate, doing modestly oscillating motions for which the reduced frequency $\sigma = \frac{1}{2}\Omega c/U < 0{\cdot}3$, where Ω is the radian frequency, c the chord-length and U the incoming velocity, wake deformation is not important. They find that, when the phase difference between pitching and heaving is $\frac{1}{2}\pi$, the pitching axis should be located, with a view to efficiency and thrust, in the rear quarter of the profile; see also Table 1 and the discussion thereof.

The influence of a uniform elasticity of the plate is that the overall instantaneous lift decreases; however, this lift is directed, by the passively bending of the plate, more in the direction of advance of the plate and by this can lead to a moderate gain of efficiency.

The analogous problem for a slender propulsor is also treated by Katz and Weihs [36].

Finally, we discuss a complementary approach for estimating the highest possible efficiency of a large-amplitude propulsive motion of a caudal fin of finite span. By this method the optimum shed vorticity is determined, so to speak, *a priori* and not by the way in which the active and/or passive flexible fin moves through the fluid.

The fish swims with a velocity U in the negative x-direction (Figure 28) and we assume the path of the trailing edge of its tail W to be known in one way or another. This path is the periodic strip H, which does not need to be flat in the y-direction, so that it can belong to, for instance, a lunate tail, and it has a large amplitude in the z-direction.

Assume that the vorticity shed by the trailing edge of the tail is small of $O(\epsilon)$ and remains where it is formed on H. This is a reasonable assumption when the reduced frequency of the motion of the tail is not too high. We want to determine the optimum shed vorticity on H and by this the highest possible efficiency of propulsion. This can be found in a simple way as is discussed for instance by Potze and Sparenberg in 'On the efficiency of optimum finite amplitude sculling propulsion' [37].

Consider the geometric strip H to be materialized, so that is becomes impermeable while its thickness is zero. Place this strip in a homogeneous flow of velocity λ parallel to the x-axis. Then vorticity $\lambda\boldsymbol{\gamma}(x, y)$ is needed on H in order for the flow not to penetrate H, which can be calculated by a vortex lattice method. The vorticity has to be chosen so that the circulation

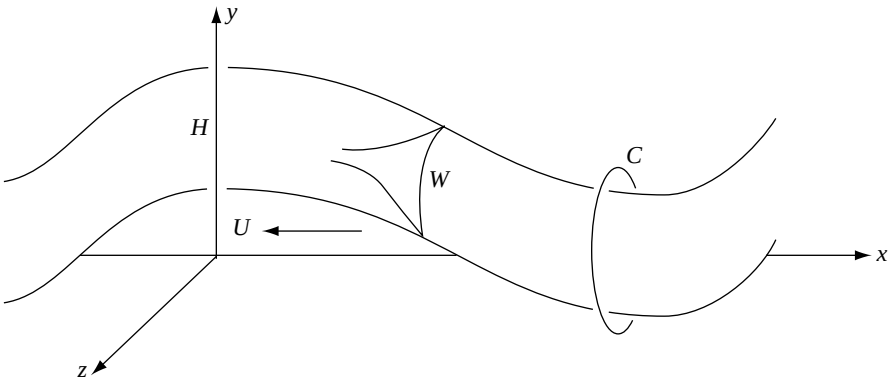

Figure 28. Strip H passed through by trailing edge of tail W.

along any contour C around H is zero because a wing moving in an undisturbed fluid can leave behind only such vorticity. Apart from the still unknown factor λ, this vorticity $\lambda\boldsymbol{\gamma}(x, y)$ is the optimum vorticity left behind on H by W.

The unknown factor λ follows from the desired mean value of the thrust $\overline{T} = O(\epsilon)$ which is directly coupled to the momentum of the fluid in the x-direction induced by $\lambda\boldsymbol{\gamma}(x, y)$, which we now assume to be present at the two-sided infinite strip H when the tail has travelled to $x = -\infty$. Indeed, $\overline{T}$ equals the mean momentum of the fluid over a length U in the x-direction by which $\lambda = O(\epsilon)$ is known.

The mean value of the kinetic energy $E = O(\epsilon^2)$ left behind over a distance U can then be calculated and the efficiency η of the propulsion becomes

$$\eta = \frac{U\overline{T}(\epsilon)}{U\overline{T}(\epsilon) + \overline{E}(\epsilon^2)} = 1 - O(\epsilon). \tag{14.2}$$

Because it is likely that a living aquatic animal will swim in an energy-saving way, it is not unlikely that the passive elasticity of the tail and its active deformations are such that this value can have a meaning.

15. Some special ways in which fish may swim

In the foregoing sections the subjects were rather fundamental regarding the hydrodynamics of the swimming of fish, *i.e.*, how a fish propels itself. In this section we mention briefly how fish swim in order to attain some specific aims. Here the word aim is used in an evolutionary sense where the behaviour of living creatures is probably the outcome of blind changes in the genes of their ancestors of which the useful ones remain and cause the survival of the fittest in relation to the momentary environment.

We start with the article 'Optimal fish cruising speed' [38] by Weihs about the speed at which a fish can cover the largest possible distance when it has a given finite amount of usable energy at its disposal. This energy has to be used for the propulsive rate of work W_p and for the rate of energy W_m needed for its internal metabolic process when the fish is at rest. Weihs considers the relation

$$E = (W_p + W_m)t, \tag{15.1}$$

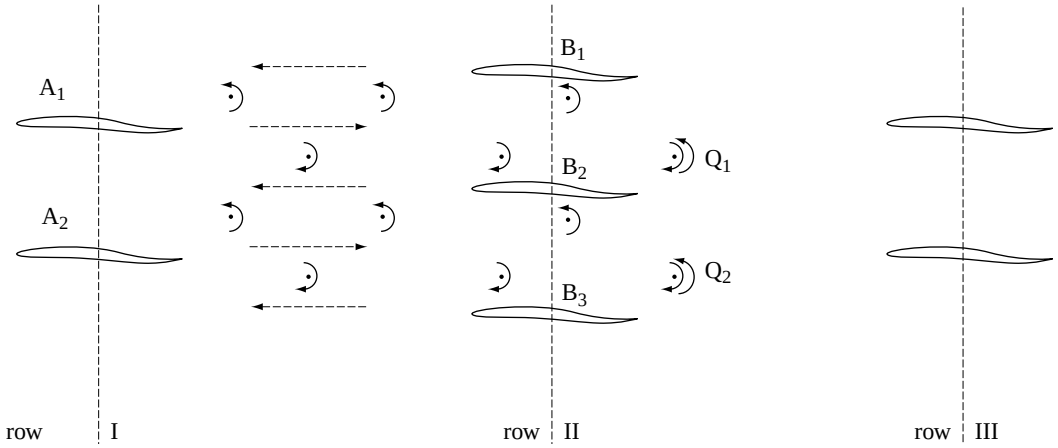

Figure 29. Scheme of in phase swimming fishes in a school. Free after Weihs.

where E is the available energy and t the total time of swimming. When T is the mean value of the thrust, u the mean velocity of swimming and τ a drag coefficient, the following realistic relation can, for instance, be assumed

$$T = \tau u^2. \tag{15.2}$$

The relation between W_p and T is formulated by means of the efficiency η of the propulsion mechanism of the fish

$$\eta W_p = Tu. \tag{15.3}$$

From experiments carried out by Webb with the rainbow trout reported in 'The swimming energetics of trout, II Oxygen consumption and swimming efficiency' [39], it was found that the relation between the efficiency η and the velocity u can, by introducing a constant β, be written as

$$\eta = \beta u. \tag{15.4}$$

When these relations are combined, it is found that the distance l that can be covered by using the given amount of available energy E becomes

$$l(u) = Eu \Big/ \left(\frac{\tau}{\beta} u^2 + W_m \right). \tag{15.5}$$

Differentiation of $l(u)$ with respect to u and by putting $\mathrm{d}l(u)/\mathrm{d}u = 0$, the optimum cruising speed u_{opt} and, by this, the optimum $W_{p,\mathrm{opt}}$ are found

$$u_{\mathrm{opt}}^2 = \frac{\beta}{\tau} W_m \rightarrow W_{p,\mathrm{opt}} = W_m. \tag{15.6}$$

Hence, under the assumptions (15.2) and (15.4) it is found that for the optimum cruising speed, the rate of energy used for the propulsion equals the rate of energy needed for the internal metabolic process at rest.

For the inverse problem, when it is asked to determine the optimum velocity $\tilde{u}_{\mathrm{opt}}$ for minimum energy expenditure for covering a prescribed distance l, it is found that $\tilde{u}_{\mathrm{opt}} = u_{\mathrm{opt}}$. This

follows from (15.5), but now with l as a given constant and $E = E(u)$, by putting $\mathrm{d}E/\mathrm{d}u = 0$. The equality of both velocities can also be argued from the meaning of the problem.

We refer to Weihs [38] for further biological applications of these results.

Next we mention the way of swimming which is called burst-and-glide or burst-and-coast swimming. The following is based on the supposition that, by the swimming movements of a fish, its drag can increase, even by a factor of 3 or more. This seems to be in contradiction with the results described in Section 5 that were obtained by a robotic model of a swimming blue fin tuna. The model had a length of 1·25 m and swam at a Reynolds number $Ul/\nu = 10^6$ and it was found that its drag decreased by its swimming motions compared to its drag when it is towed through the water as a rigid body. However, when smaller fish are considered, by swimming at another Reynolds number, it is perhaps possible, as many authors believe and can defend, that there will be an increase of drag by the swimming motions. Then the burst-and-glide procedure yields a way of avoiding this higher drag to a certain extent.

This was investigated in the paper 'Energetic advances of burst swimming of fish' [40] by Weihs. He considers the following periodic behaviour of the fish. A swimming period starts with a relatively large thrust T during a time interval $(0 - t_1)$ by which the fish is accelerated from a velocity U_i to a velocity U_f. Then the propulsive motion of the fish stops, so that the thrust is zero and the fish glides as a rigid body, while by its drag the velocity decreases from U_f again to U_i at the moment $(t_1 + t_2)$ when a new period starts.

During the accelerating phase energy is used and the velocity increases, by which the efficiency of the propulsion η also increases (15.4), while the drag of the strongly squirming fish is assumed to be large. Here, however, a result of Section 5 below point (5) can play an interesting part. There it was measured that, by extra thrust production, which is possibly related to the acceleration here, a drag reduction of more than 70% can occur, instead of the assumed increase. Then, instead of an unfavourable acceleration motion, a favourable one would occur.

After the acceleration follows the gliding as a rigid body during which no energy is used and the drag is assumed to be small. By using some assumptions, (15.4) is one of these, Weihs calculates the mean energy used per unit of length for this type of periodic propulsion and compares this with the energy needed per unit of length when the fish swims with a constant velocity equal to the mean velocity of the burst-and-glide procedure.

He arrives at the conclusion that it can happen theoretically that by burst-and-glide swimming only 54% of the energy necessary for swimming with the above mentioned constant mean velocity is needed.

We will mention yet another way of swimming, namely the schooling of fish. Schooling fish swim in a strikingly well-arranged formation. In his article 'Hydromechanics of fish schooling' [41] Weihs discusses the swimming in phase of a two-dimensional school of fish in a shallow-water basin. Then the vorticity shed by the tails of the fish can be considered approximately as short concentrated vertical vortex lines ending at the bottom of the basin and at the surface of the water; Figure 29.

Straight behind fish A_2 the fluid flow induced by its alternatingly shed vortices has components opposite to the swimming direction of the fish, while outside these vortices the induced flow has a component in the swimming direction; see the dashed vectors in between rows I and II. So a fish B_2 of row II can better choose its swimming position in between his predecessors A_1 and A_2 of row I. By a correct spacing, the fish of row II can, to some extent, destroy the vortices of the fish of row I, points Q_1 and Q_2. This can be helpful for the fish in row III which then have a less disturbed incoming flow.

Quite a different approach to the investigation of schooling is used in 'Models for tuna school formation' [42] by Stöcker where a so-called automaton model is considered that has general application, as the author states, to complex configurations of animals in motion. There a two-dimensional cellular space is introduced in which, in the case of schooling, in each cell a number $(0, 1, 2, \ldots)$ of fish can be present that migrate to neighbouring cells by means of suitably chosen rules. These rules can be based on the induced velocity fields by neighbouring fishes or even on oxygen depletion by which a school will break up. Then, after a number of time steps (as large as 2000), schooling formations can arise.

16. Acknowledgment

The author thanks his collague Prof. Dr. B.L.J. Braaksma for some discussions about the theory of analytic functions. He is also grateful to the referees for mentioning additonal references, for valuable remarks and for indicating inaccuracies in the script.

References

1. M. Yousuff Husaini (ed.), *Collected Works of Sir James Lighthill*. New York: Oxford University Press (1996) 532 pp.
2. R.McN. Alexander, The history of fish mechanics. In: P.W. Webb and D. Weihs (eds.), *Fish Biomechanics*. New York: Praeger Press (1983) 1–35.
3. C.M. Breder, The locomotion of fishes. *Zoologica* 4 (1926) 159–256.
4. R.W. Blake, *Fish Locomotion*. Cambridge: Cambridge University Press (1983) 208 pp.
5. G.I. Taylor, Analysis of the swimming of long and narrow animals. *Proc. R. Soc. London* A214 (1952) 158–183.
6. M.J. Lighthill, Note on the swimming of slender fish. *J. Fluid Mech.* 9 (1960) 305–317.
7. T.Y. Wu, Swimming of a waving plate. *J. Fluid Mech.* 10 (1961) 321–344.
8. J.A. Sparenberg, *Hydrodynamic Propulsion and Its Optimization*. Dordrecht: Kluwer Academic Publishers (1995) 365 pp.
9. P.G. Saffman, The self propulsion of a deformable body in a perfect fluid. *J. Fluid Mech* 28 (1967) 385–389.
10. J. Gray, Studies in animal locomotion VI: The propulsive powers of the dolphin. *J. Exp. Biol*. 13 (1936) 192–199.
11. M.J. Lighthill, Large amplitude elongated body theory of fish locomotion. *Proc. R. Soc. London* B179 (1971) 125–138.
12. D.S. Barret, M.S. Triantafyllou, D.K.P. Yue, M.A. Grosenbaugh and M.J. Wolfgang, Drag reduction in fish-like locomotion. *J. Fluid Mech.* 392 (1999) 183–212.
13. R. Coene, Notes on the efficiency of propulsion of bodies in waves. *J. Fluid Mech.* 153 (1985) 103–122.
14. M.J. Lighthill, Aquatic animal propulsion of high hydromechanical efficiency. *Ann. Rev. Fluid Mech.* 1 (1970) 413–446.
15. W.S. Childress, *Mechanics of Swimming and Flying*. New York: Courant Institute of Mathematical Sciences (1977).
16. C.S. Wardle and A. Reid, The application of large amplitude elongated body theory to measure swimming power in fish. In: T.J. Pedley (ed.), *Scale Effects in Animal Motion*. New York: Academic Press (1977) pp. 299–313.
17. M.J. Lighthill and R.W. Blake, Biofluid dynamics of balistiform and gymnotiform locomotion. Part 1, Biological background and analysis by elongated-body theory. *J. Fluid Mech.* 212 (1990) 183–207.
18. M.J. Lighthill, Biofluid dynamics of balistiform and gymnotiform locomotion. Part 2. The pressure distribution arising in two-dimensional irrotational flow from a general motion of a flexible plate normal to itself. Part 3. Momentum enhancement in the presence of a body of elliptical cross-section. Part 4. Short wavelength limitations on momentum enhancement. *J. Fluid Mech.* 213 (1990) 1–28.
19. T.Y. Wu, Hydrodynamics of swimming propulsion. Part 1. Swimming of a two-dimensional flexible plate at variable forward speeds in an inviscid fluid. Part 2. Some optimum shape problems. Part 3. Swimming and

optimum motions of slender fish with side fins. *J. Fluid Mech.* 46 (1971) Part 1, 337–355; Part 2, 521–544; Part 3, 545–568.
20. T.Y. Wu and J.N. Newman, Unsteady flow around a slender fish-like body. *J. Mech. Eng. Sci.* 14 (1972) N7.
21. N.J. Muskhelishvili, *Singular Integral Equations*. Groningen: P. Noordhoff N.V. (1953).
22. J.N. Newman and T.Y. Wu, A generalized slender-body theory for fish-like forms. *J. Fluid Mech.* 57 (1973) 673–693.
23. J.N. Newman, The force on a slender fish-like body. *J. Fluid Mech.* 58 (1973) 689–702.
24. T.Y. Wu and A.T. Chwang, Extraction of flow energy by fish and birds in a wavy stream. In: T.Y. Wu, C.J. Brokaw and C. Brennen (eds.) *Swimming and Flying in Nature*, Vol. 2. New York: Plenum Press (1974) pp. 687–702.
25. H.P. Urbach, Existence of optimum propulsion by means of periodic motions of a rigid profile. *Studies App. Math.* 81 (1989) 93–116.
26. H.P. Urbach, On optimum propulsion by means of small periodic motions of a rigid profile, I. Properties of optimum motions, II. Optimization of the period and numerical results. *Studies App. Math.* 82 (1990) I 121–180, II 181–215.
27. D.G. Luenberger, *Optimization by Vector Space Methods*. New York: John Wiley and sons (1969).
28. M.J. Lighthill, Hydromechanics of aquatic propulsion: a survey. *Ann. Rev. Fluid Mech.* 1 (1969) 413–446.
29. M.G. Chopra and T. Kambe, Hydrodynamics of lunate tail swimming propulsion. Part 2. *J. Fluid Mech.* 79 (1977) 46–69.
30. G. Karpouzian, G. Spedding and H.K. Cheng, Lunate tail swimming propulsion, Part 2, Performance analysis. *J. Fluid Mech.* 210 (1990) 329–351.
31. C.P. van Dam, Efficiency characteristics of crescent shaped wings and caudal fins. *Nature* 325 (1987) Letters to Nature.
32. J. Ashenberg and D. Weihs, Curved lifting line theory for thin planar wings. *Israel J. Techn.* 20 (1982) 160–165.
33. J. Ashenberg and D. Weihs, Minimum induced drag of wings with curved planform. *J. Aircraft* 21 (1984) 89–91.
34. J.Y. Cheng, L.X. Zhuang and B.G. Tong, Analysis of swimming three-dimensional waving plates. *J. Fluid Mech.* 232 (1991) 341–355.
35. J. Katz and D. Weihs, Hydrodynamic propulsion by large amplitude oscillation of an airfoil with chordwise flexibility. *J. Fluid Mech.* 88 (1978) 485–497.
36. J. Katz and D. Weihs, Large amplitude unsteady motion of a flexible slender propulsor. *J. Fluid Mech.* 90 (1979) 713–723.
37. W. Potze and J.A. Sparenberg, On the efficiency of optimum finite amplitude sculling propulsion. *Int. Shipbuilding Progress* 30 (1983) 238–244.
38. D. Weihs, Optimal fish cruising speed. *Nature* 245 (1973) 48–50.
39. P.W. Webb, The swimming energetics of trout II. Oxygen consumption and swimming efficiency. *J. Exp. Biol.* 55 (1971) 521–540.
40. D. Weihs, Energetic advances of burst swimming of fish. *J. Theor. Biol.* 48 (1974) 215–229.
41. D. Weihs, Hydromechanics of fish scooling. *Nature* 241 (1973) 290–291.
42. S. Stöcker, Models for tuna school formation. Math. Biosci. 156 (1999) 167–190.